Geol. Mag. **154** (*2*), *2017, pp. 354–380.* © *Cambridge University Press 2016*
doi:10.1017/S0016756816000030

Rapid extensional unroofing of a granite–migmatite dome with relics of high-pressure rocks, the Podolsko complex, Bohemian Massif

JIŘÍ ŽÁK*†, JIŘÍ SLÁMA‡ & MIROSLAV BURJAK*§

*Institute of Geology and Paleontology, Faculty of Science, Charles University, Albertov 6, Prague, 12843, Czech Republic
‡Institute of Geology, Czech Academy of Sciences, Rozvojová 269, Prague, 16500, Czech Republic
§Geotest, PLC, Olšanská 3, Prague, 13000, Czech Republic

(*Received* 11 October 2015; *accepted* 6 January 2016; *first published online* 11 February 2016)

Abstract – The Podolsko complex, Bohemian Massif, is a high-grade dome that is exposed along the suprastructure–infrastructure boundary of the Variscan orogen and records snapshots of its protracted evolution. The dome is cored by leucocratic migmatites and anatectic granites that enclose relics of high- to ultrahigh-pressure rocks and is mantled by biotite migmatites and paragneisses whose degree of anatexis decreases outwards. Our new U–Pb zircon ages indicate that the leucocratic migmatites were derived from Early Ordovician (*c.* 480 Ma) felsic igneous crust; the same age is inferred for melting the proto-source of the metapelitic migmatites. The relics of high- to ultrahigh-pressure rocks suggest that at least some portions of the complex witnessed an early Variscan subduction to mantle depths, followed by high-temperature anatexis and syntectonic growth of the Podolsko dome in the middle crust at *c.* 340–339 Ma. Subsequently, the dome exhumation was accommodated by crustal-scale extensional detachments. Similar *c.* 340 Ma ages have also been reported from other segments of the Variscan belt, yet the significance of this tectonothermal event remains uncertain. Here we conclude that the 340 Ma age post-dates the high-pressure metamorphism; the high temperatures required to cause the observed isotopic resetting and new growth of zircon were probably caused by heat input from the underlying mantle and, finally, the extensional unroofing of the complex requires a minimum throw of about 8–10 km. We use this as an argument for significant early Carboniferous palaeotopography in the interior of the Variscan orogen.

Keywords: anisotropy of magnetic susceptibility (AMS), granite–migmatite dome, exhumation, metamorphic core complex, U–Pb zircon geochronology.

1. Introduction

It has long been recognized that ancient collisional orogens commonly consist of high-grade 'axial' zones surrounded by upper crust, often referred to as the infrastructure and superstructure, respectively (e.g. de Sitter & Zwart, 1960; Zwart, 1967; Murphy, 1987; Carreras & Capella, 1994; Culshaw, Beaumont & Jamieson, 2006), or plateau and foreland in other concepts (e.g. Rey, Teyssier & Whitney 2010; Whitney *et al.* 2015). Most recent models attempting to explain the tectonic juxtaposition of such contrasting crustal levels invoke displacement on low- to moderate-angle extensional detachments (e.g. Dewey, 1988; Costa & Rey, 1995; Rey, Vanderhaeghe & Teyssier, 2001; Platt *et al.* 2003; Rivers, 2012; Whitney *et al.* 2013; Platt, Behr & Cooper, 2014) and channel flow and extrusion of ductile lower crust between an underthrust continental indenter and an overlying upper-crustal rigid lid (e.g. Beaumont *et al.* 2001; Jamieson & Beaumont, 2013).

†Author for correspondence: jirizak@natur.cuni.cz

An important feature of orogenic infrastructure is the presence of high-pressure to ultrahigh-pressure (HP–UHP) rocks that commonly occur as small lenses or layers within relatively lower-pressure, mid-crustal host (see Dobrzhinetskaya & Faryad, 2011; Liou *et al.* 2014 for overviews). The significance of such even volumetrically minor and sparse relics of HP–UHP rocks in the reconstruction of the tectonic evolution of collisional orogens is enormous as they may preserve the only record of an early subduction history of the orogen. In some cases, the HP–UHP assemblages tend to delineate the suprastructure–infrastructure boundary, raising the issue of how they were exhumed from the base of the thickened crust or even from mantle depths to shallow levels in these specific tectonic settings.

This paper examines the Podolsko complex, Bohemian Massif, as an example of a high-grade granite–migmatite dome that encloses relics of HP–UHP rocks and has been exhumed along the suprastructure–infrastructure boundary of the Variscan orogen (Fig. 1). New field observations and structural and anisotropy

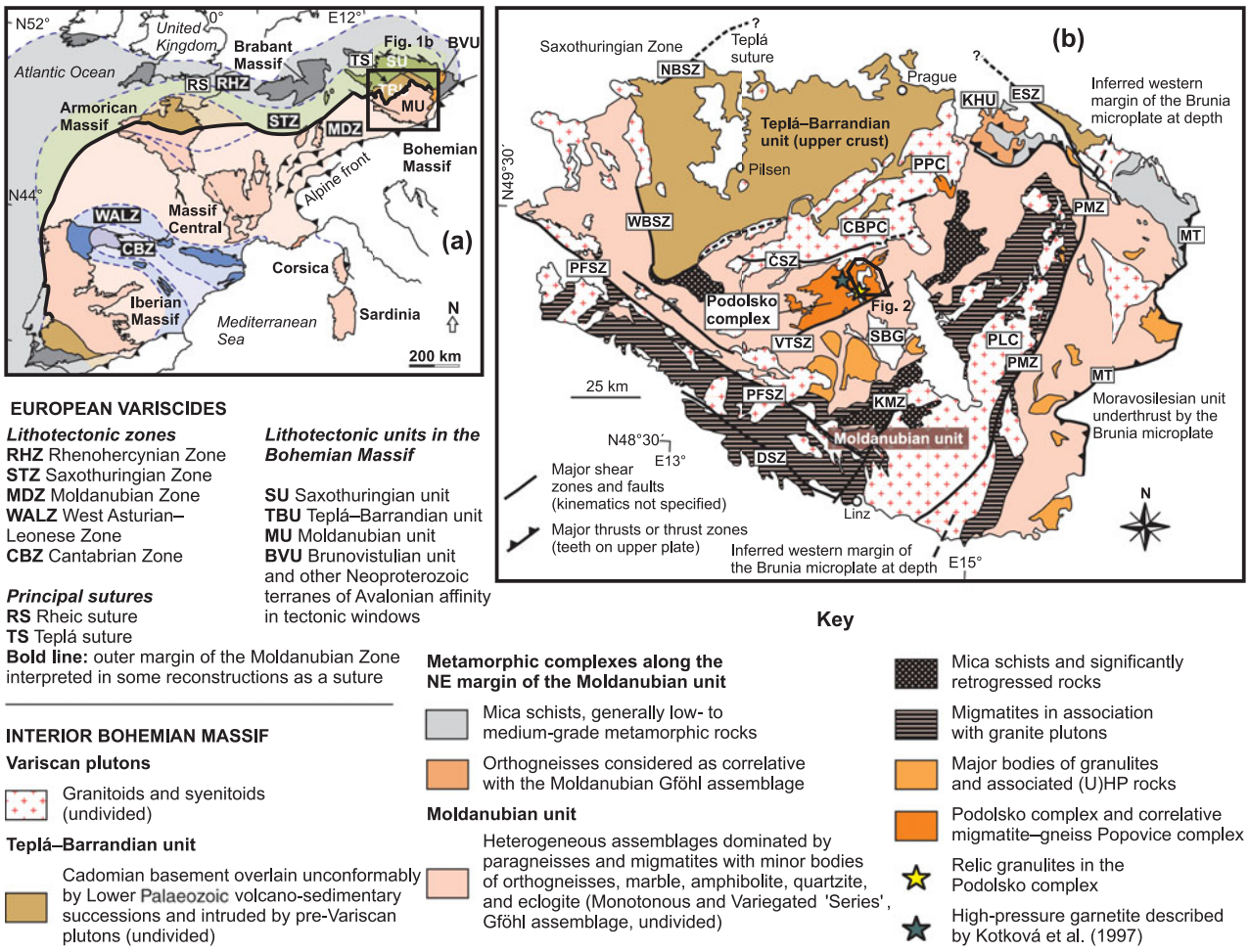

Figure 1. (Colour online) (a) Overview geological map showing basement outcrop areas and principal lithotectonic zones and sutures of the Variscan orogenic belt in Europe. Bohemian Massif is the easternmost inlier of the orogen. Compiled from Winchester (2002), Asch (2003) and Martínez Catalán (2011, 2012). (b) Greatly simplified geological map of the interior Bohemian Massif emphasizing orogenic suprastructure as represented by the Teplá–Barrandian unit and exhumed infrastructure (Moldanubian unit). The Podolsko complex is exposed near the suprastructure–infrastructure boundary. Based on geological map of the Czech Republic 1:500,000 published by the Czech Geological Survey, Prague. Principal lithotectonic elements and shear zones: CBPC – Central Bohemian Plutonic Complex; ČSZ – Červená shear zone; ESZ – Elbe shear zone; DSZ – Danube shear zone; KHU – Kutná Hora unit; KMZ – Kaplice mica schist zone; MT – Moldanubian thrust; NBSZ – North Bohemian shear zone; PFSZ – Pfahl shear zone; PLC – Pelhřimov complex; PMZ – Přibyslav mylonite zone; PPC – Popovice complex; SBG – South Bohemian granulites; VTSZ – Vodňany–Týn nad Vltavou shear zone; WBSZ – West Bohemian shear zone.

of magnetic susceptibility (AMS) data are presented, together with high-precision U–Pb zircon ages obtained using laser-ablation inductively coupled plasma mass spectrometry (LA-ICP-MS) to reveal the previously poorly known tectonic history of this metamorphic complex. Based on a combination of these datasets, we then argue for at least a three-stage exhumation history of the mixed (U)HP–mid-crustal assemblage, with late stages being facilitated firstly by lateral shortening and then by the supracrustal–infracrustal boundary as a major extensional detachment at around 340 Ma. This age has been particularly important for the evolution of the Variscan orogenic belt: it has been recognized in various parts of the orogen across central, western and southern Europe and is thought to represent a major changeover in its thermal–mechanical development. In this context, we finally add some new constraints and discuss the geodynamic significance of this *c.* 340 Ma tectonothermal event.

2. Plate-tectonic setting of the Podolsko complex

The Bohemian Massif of central Europe is the easternmost inlier of the once continuous but now largely dismembered Ouachita–Appalachian–Variscan orogenic belt that formed during the Devonian–Carboniferous convergence of Gondwana and Laurussia (Fig. 1; e.g. Pharaoh, 1999; Tait *et al.* 2000; Matte, 2001; Winchester, 2002; Winchester *et al.* 2006; Nance *et al.* 2010; Kroner & Romer, 2013). A characteristic feature of the Variscan orogeny was the involvement of a number of microplates that were stuck in a broad collision zone as the two supercontinents converged, resulting in multiple subduction, accretion and collision events along the margins of the neighbouring microplates. As a result, the Bohemian Massif is a mosaic of several lithospheric units that have been variously correlated with broadly similar units across Western Europe to define three main zones of the orogen:

https://doi.org/10.1017/S0016756816000030 Published online by Cambridge University Press

Rhenohercynian, Saxothuringian and Moldanubian (Fig. 1).

One of the most important lithotectonic boundaries in the Variscan orogen delineates the outer margin of the Moldanubian Zone (Fig. 1) and separates generally low-grade, upper-crustal from high-grade, mid- to lower-crustal units representing orogenic suprastructure and infrastructure, respectively. The nature of this boundary varies along the strike of the orogen and the boundary records a complex polyphase history as proposed, for instance, by Skrzypek *et al.* (2014) for the Vosges Mountains and by Ballévre *et al.* (2009) for the Armorican Massif in France (Fig. 1a). The same also applies to the Bohemian Massif: almost every possible sense of movement has been invoked to explain kinematic evolution of the SE boundary between the upper crust represented by the Teplá–Barrandian unit and the mid- to lower-crustal Moldanubian unit. The existing interpretations of their juxtaposition include: (1) dextral strike-slip shearing during early Carboniferous time (Matte *et al.* 1990); (2) sinistral strike-slip faulting at *c.* 320 Ma (Pitra, Burg & Guiraud, 1999); (3) top-to-the-SE thrusting of the Teplá–Barrandian over Moldanubian (Košler *et al.* 1995); (4) normal movements (Teplá–Barrandian down, Moldanubian up) (Pitra *et al.* 1994; Zulauf, 1994; Scheuvens & Zulauf 2000; Dörr & Zulauf, 2010); (5) polyphase evolution involving *c.* 380–365 Ma sinistral transtension, *c.* 354–346 Ma horizontal shortening and dextral transpression and *c.* 346–337 Ma normal movements (Žák *et al.* 2014; Tomek, Žák & Chadima, 2015).

The importance of the Teplá–Barrandian/Moldanubian boundary for understanding the evolution of the Variscan orogen is outstanding, with its plate-tectonic and palaeogeographic significance being vigorously debated. In one viewpoint, the boundary has been interpreted as a suture left behind after an oceanic domain subducted beneath the Teplá–Barrandian and which is now separating the outboard Cadomian terranes from the inboard Gondwana mainland (e.g. Franke, 1999). In an opposing view, the Teplá–Barrandian and Moldanubian units represent different structural levels of a single microplate and therefore no suture is implied (e.g. Schulmann *et al.* 2014).

Consequently, the palaeogeographic and tectonic significance of the Moldanubian unit, characterized by a complex and protracted Variscan tectonometamorphic history, remains uncertain (see Finger *et al.* 2007; Lardeaux *et al.* 2014 for overviews). Large portions of this unit have pre-Variscan siliciclastic (meta-)sedimentary protoliths and are now represented by the low-pressure–high-temperature (LP–HT), commonly cordierite- and sillimanite-bearing and migmatitic biotite paragneisses, traditionally termed the Monotonous 'series' (e.g. Linner, 1996; Petrakakis 1997; René, 2006). The metaclastic rocks host numerous scattered kilometre-scale bodies of orthogneisses with Cambro-Ordovician protolith ages (Klomínský, Jarchovský & Rajpoot, 2010), whereas other metasedimentary complexes enclose abundant lenses of marble, calc-silicate rocks, amphibolite and quartzite (the Varied 'series'). The Moldanubian unit also contains multiple bodies of migmatitic orthogneisses and granulite facies rocks with intercalations of mantle peridotites, eclogites and pyroxenites, collectively referred to as 'the Gföhl assemblage' (Fig. 1b; e.g. Carswell & O'Brien, 1993; O'Brien & Carswell, 1993; Owen & Dostal, 1996; Cooke & O'Brien, 2001; Medaris *et al.* 2005; Medaris, Beard & Jelínek, 2006; Kotková, 2007). Since the seminal paper by Tollmann (1982), the large-scale structure of the Moldanubian unit has been interpreted as a result of nappe stacking where the highest-grade Gföhl assemblage was thrust to the SE as a coherent subhorizontal nappe over the underlying, lower-grade Varied and Monotonous 'series' (e.g. Matte *et al.* 1990; Franke, 2000, 2006). This assessment has been largely abandoned in a number of modern structural studies in favour of crustal-scale buckling, leading to vertical exhumation of high-pressure rocks followed by mid-crustal horizontal channel flow (e.g. Franěk, Schulmann & Lexa, 2006; Franěk *et al.* 2011). Based on lithologic similarities, the Podolsko complex has also been assigned to the Gföhl assemblage and should even correspond to a root zone of the Gföhl nappe located along the Teplá–Barrandian/Moldanubian boundary. This point is returned to in the Discussion (Section 7).

3. Geology of the Podolsko complex and its mantling rocks

This paper concentrates on the NE portion of the Podolsko complex and its mantling rocks, both superbly exposed along the canyons of the Vltava and Lužnice rivers (Fig. 2). Other portions of the complex are poorly exposed or concealed beneath sedimentary cover. To the north, the Podolsko complex has been intruded along a sheeted contact by granitoids and melasyenitoids of the upper-crustal Central Bohemian Plutonic Complex with an estimated emplacement depth of *c.* 8–10 km (Žák *et al.* 2012). The granitoids have been pervasively deformed in a magmatic to solid state along a major extensional detachment, the Červená shear zone, dipping moderately to the NNW (beneath the pluton). The detachment is one segment of several interconnected normal shear zones that delineate the Teplá–Barrandian upper crust and accommodated its downdrop and exhumation of the Moldanubian unit from *c.* 346 Ma to *c.* 337 Ma (main phase of ductile movements; Fig. 1b; Žák, Holub & Verner, 2005; Dörr & Zulauf, 2010). The Podolsko complex is exposed in the footwall of the Červená shear zone and is therefore directly juxtaposed with the upper crust (Fig. 2).

The complex itself is dominated by leucocratic migmatites, granitic gneisses and anatectic biotite granites, with a few minor bodies of variably retrogressed felsic kyanite-bearing and mafic orthopyroxene granulites and serpentinites (Zelenka, 1927; Urban, 1930; Röhlichová, 1962, 1963; Fediuková & Fediuk, 1971).

https://doi.org/10.1017/S0016756816000030 Published online by Cambridge University Press

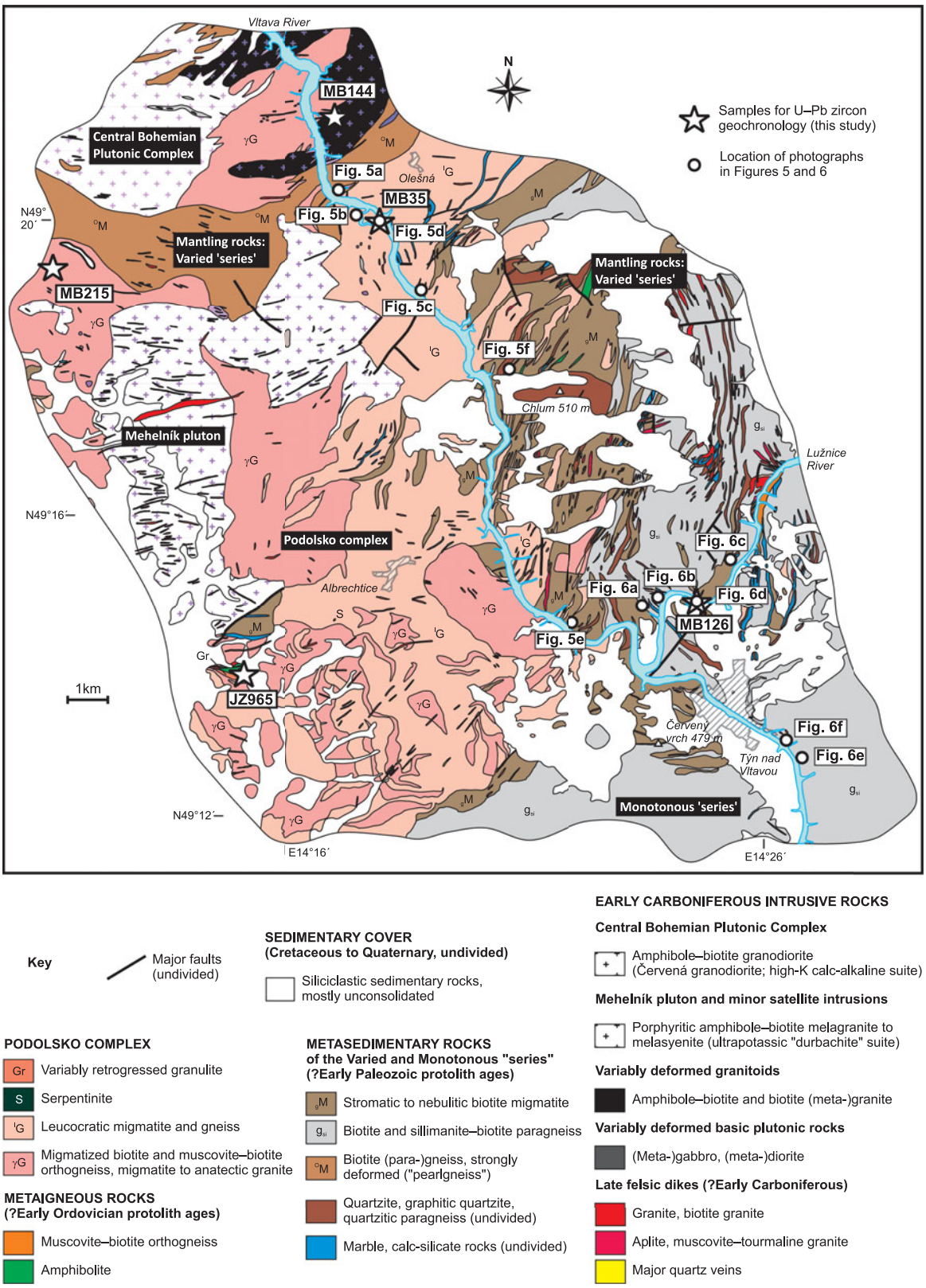

Figure 2. (Colour online) Detailed geological map of the eastern part of the Podolsko complex and its mantling metasedimentary rocks. Compiled from Czech Geological Survey maps, scale 1:25,000, sheets 22–412 Záhoří, 22–121 Bechyně, 22–414 Protivín and 22–423 Týn nad Vltavou.

Fišera, Vrána & Kotrba (1982) were the first to interpret the granulites as recording a three-stage metamorphic history from a HP event through granulite facies overprint to extensive migmatization at lower pressures. These findings were corroborated by Kotková, Harley & Fišera (1997), who reported blocks of crustally derived garnetite that recorded UHP conditions with a pressure of *c.* 2.8 GPa at a temperature of *c.* 830 °C (based on garnet–orthopyroxene geothermobarometry) and later granulite-facies overprint at a pressure of *c.*

https://doi.org/10.1017/S0016756816000030 Published online by Cambridge University Press

0.8 GPa (see also Krenn & Finger, 2004; Finger & Krenn, 2007). The existing petrologic studies therefore indicate that at least some portions of the Podolsko complex were subducted to mantle depths and then decompressed to granulite-facies conditions.

Kotková, Dörr & Finger (1998) also obtained a poorly constrained $^{207}Pb/^{206}Pb$ age of 360 ± 10 Ma on zircons and a total Pb age of 341 ± 15 Ma on monazite from this sample. These ages broadly overlap with those reported by Finger & Krenn (2007), who provided a chemical Th–U–Pb age of 341 ± 7 Ma on monazite to date the (U)HP stage. The above studies and geological mapping also agreed that the complex experienced polyphase deformation and metamorphism during Late Devonian – early Carboniferous times.

The Podolsko complex has been intruded by variably sized bodies of ultrapotassic melagranites to melasyenites (*c.* 343–337 Ma durbachite suite) (Holub, 1997; Holub, Cocherie & Rossi, 1997; Janoušek & Gerdes, 2003) and numerous dykes of biotite and tourmaline granite, aplite and pegmatite (Fig. 2).

To the east, the Podolsko complex is in contact with stromatic biotite migmatites containing abundant up-to-kilometre-scale intercalations of quartzites, amphibolites, marbles and calc-silicate rocks, the whole assemblage being assigned to the Varied 'series' (Fig. 2). The contact between the Podolsko complex and metasedimentary rocks is not sharp-planar; instead, the Podolsko migmatites are interfingered with and form thin isolated lenses within the metasedimentary rocks. Vice versa, the metasedimentary rocks form abundant isolated screens within the leucocratic migmatites (Fig. 2).

To the south, both the Podolsko complex and the Varied unit have been overprinted by a broad *c.* NNW-dipping ductile normal shear zone (the Vodňany–Týn nad Vltavou shear zone) which truncates the complex, deflects the *c.* N–S-trending lithologic boundaries in the Varied 'series', and juxtaposes these units with pervasively sheared and variably retrogressed sillimanite–biotite paragneisses of the Monotonous 'series' in the footwall (Fig. 2). This shear zone was also termed the 'Podolsko detachment' by Lobkowicz, Štědrá & Schulmann (1996) and interpreted as recording extensional collapse in the interior of the Variscan orogen.

4. Structural analysis of the Podolsko complex and its mantling rocks

4.a. Mesoscopic fabrics

Across the Podolsko complex in a NW–SE direction, five structural domains have been identified on the basis of degree of anatexis, fabric orientation, fabric ellipsoid shape and kinematics (Figs 3–6).

(1) The NW sheeted contact with the *c.* 346 Ma granodiorites is a major normal, SE-side-up shear zone (the Červená shear zone) that records down-temperature deformation from magmatic to solid state under the greenschist facies conditions (Žák *et al.* 2012). The shear-zone solid-state foliation dips to the NW at a moderate angle and bears a downdip to dip-oblique, N-plunging stretching and mineral lineation (Figs 3, 4, 5a, b). The solid-state shear-zone fabric is seen in the granitoids, mantling paragneisses and leucocratic migmatites of the Podolsko complex (Fig. 3).

(2) A central domain occupied by the leucocratic migmatites is dominated by a syn-anatexis flat-lying, typically weakly developed compositional banding and biotite foliation (Figs 3, 4, 5b–d). Lineation is macroscopically not discernible on most outcrops; the macroscopic fabric ellipsoid is therefore oblate. The flat-lying foliation is superposed on an earlier *c.* NNW–SSE-trending relic steep foliation and the foliation poles therefore define a broad girdle about a gently *c.* NNW-plunging axis (Fig. 3). The flat-lying foliation has been affected by minor asymmetric s-shaped folds. The folds are gently inclined to recumbent with axial planes dipping to the *c.* SE (Fig. 5b). Although they occur domainally throughout the leucocratic migmatites, they become particularly abundant below the Červená shear zone. The fold asymmetry is consistent with the asymmetry of decimetre- to metre-scale boudins seen in places within the flat-lying foliation, both indicating normal, SE-side-up kinematics (Fig. 5c).

(3) In contrast, the easterly mantling migmatites exhibit *c.* N–S to *c.* NNE–SSW-trending steep to moderately dipping compositional banding and biotite foliation on most outcrops (Figs 3, 4, 5e, f). Again, lineation is not developed and the macroscopic fabric ellipsoid is oblate. Locally, the steep fabric is affected by minor recumbent folds with geometry similar to that observed in the leucocratic migmatites (Fig. 5e).

(4) Further to the east, the degree of anatexis decreases significantly and the syn-anatexis steep oblate fabric changes to solid-state plane-strain to strongly constrictional fabric in the outer mantling metasedimentary rocks. This fabric is defined by a strong subhorizontal *c.* NNW–SSE to *c.* N–S-trending mineral lineation and a N–S-trending foliation that dips at variable angles to the *c.* W and *c.* WSW, but is also frequently folded about a lineation-parallel axis into variably shaped minor folds (Figs 3, 4, 6a, b).

(5) To the SE, the above fabrics become pervasively overprinted by the Vodňany–Týn nad Vltavou shear zone, the fabric of which is similar to that of the northerly Červená shear zone. The shear zone foliation dips to the *c.* N to *c.* NNW at moderate angles and is associated with a dip-oblique NW-plunging mineral lineation, defined mostly by stretched sillimanite, biotite and chlorite aggregates (Figs 3, 4). Abundant macro- and microscopic kinematic indicators (asymmetric aggregates, boudins, σ-type porphyroclasts, mica fish, and anastomosing and oblique subfabrics) consistently indicate normal, SE-side-up kinematics (Fig. 6c–f).

4.b. Magmatic sheets cross-cutting the Podolsko complex

A number of magmatic sheets (dykes and sills) intruded the Podolsko complex and its mantling

https://doi.org/10.1017/S0016756816000030 Published online by Cambridge University Press

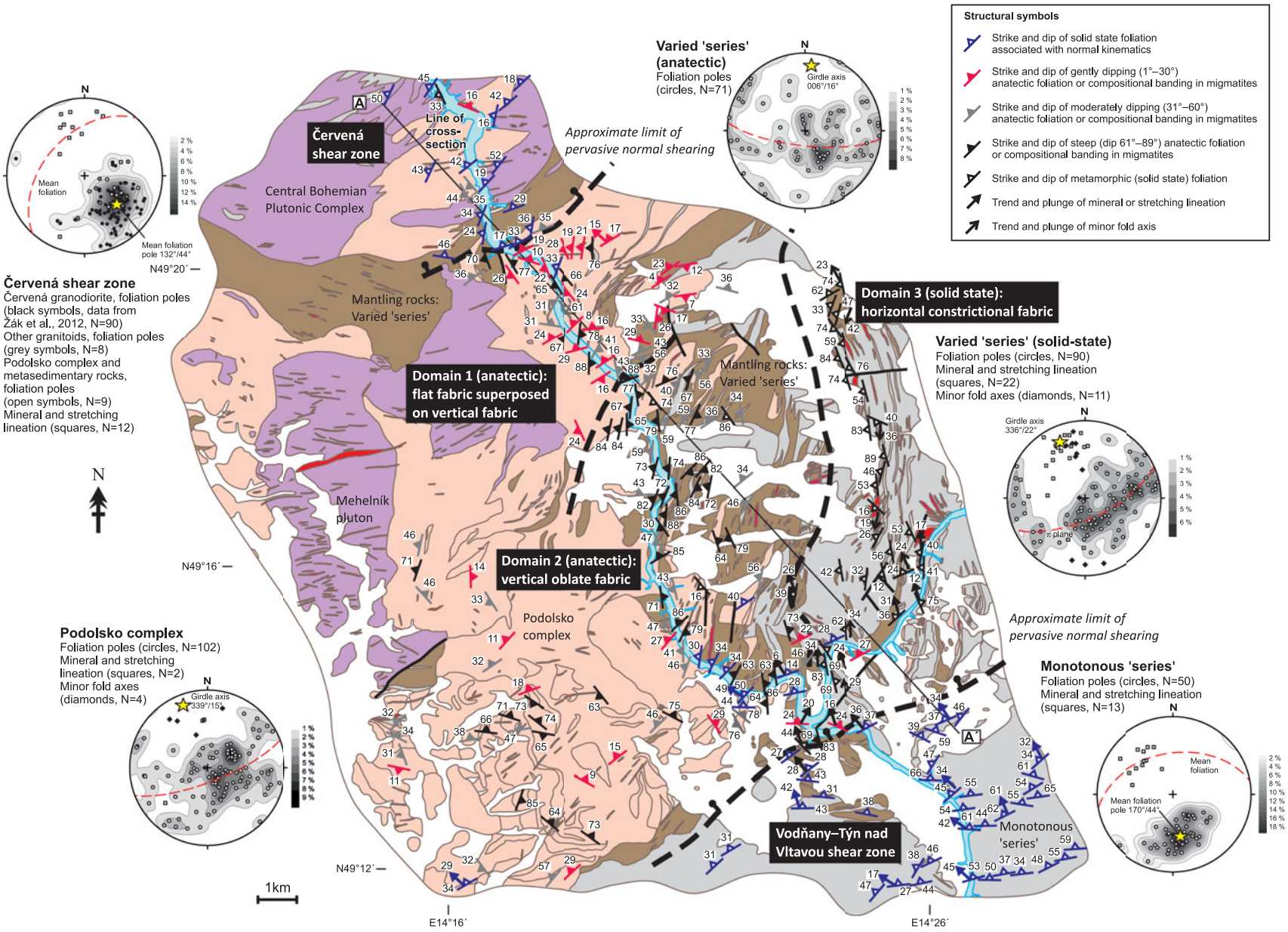

Figure 3. (Colour online) Structural map of the eastern part of the Podolsko complex and its mantling metasedimentary rocks (background same as in Fig. 2). Stereonets (equal area, lower-hemisphere projections) show orientations of main structural elements.

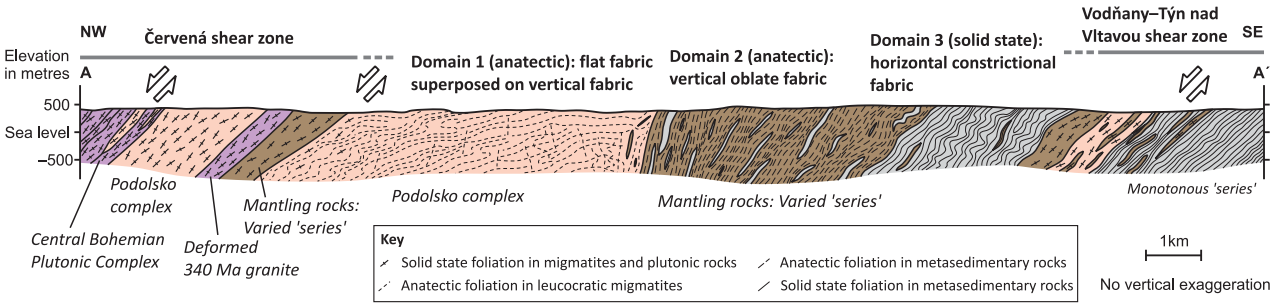

Figure 4. (Colour online) Idealized structural cross-section along line A–A´ (location shown in Fig. 3) across the eastern part of the Podolsko complex and its mantling metasedimentary rocks.

metasedimentary rocks. Their composition mostly includes melasyenite, biotite granite, aplite and muscovite–tourmaline granite (Fig. 2). On the map, the sheets have two distinct orientations. They strike *c.* N–S to *c.* NNE–SSW in the easterly mantling rocks, that is, roughly parallel to the strike of the compositional banding and metamorphic foliation, whereas they strike *c.* E–W to *c.* WSW–ENE in the Podolsko migmatites, anatectic granites and melasyenite pluton (Fig. 7). A statistical analysis of the latter sheets underlines their unimodal orientation distribution, as is apparent from the map, clustered about a mean trend of 82° (262°; Fig. 7).

5. Anisotropy of magnetic susceptibility (AMS)

5.a. Methodology

The anisotropy of magnetic susceptibility (AMS; see Hrouda, 1982; Rochette, Jackson & Aubourg, 1992; Tarling & Hrouda, 1993; Borradaile & Henry, 1997; Borradaile & Jackson, 2010 for reviews and principles of the method) was used to complement the structural data from the Podolsko complex and its mantling metasedimentary rocks. In particular, this method is useful to infer the possible principal stretching directions in migmatites which otherwise lack macroscopically discernible lineation (e.g. Ferré *et al.* 2002; Charles, Faure & Chen, 2009; Schulmann *et al.* 2009*a*; Kruckenberg *et al.* 2010, 2011; Viegas, Archanjo & Vauchez, 2013). The samples were drilled *in situ* using a hand-held gasoline drill at 35 stations (19 in the Podolsko complex, 14 in metapelitic rocks of the Varied 'series' and 2 in the variably deformed granites). A total of 80 oriented cores were cut to 404 standard cylinder-shaped specimens 10 cm^3 in volume. The AMS was measured at a low field of 200 Am^{-1} using a MFK1-A Kappabridge in the Laboratory of Rock Magnetism, Institute of Geology and Palaeontology, Charles University in Prague. A statistical analysis of the data was carried out using the ANISOFT 4.2 software (www.agico.com). The measured data are presented in Figure 8 and listed in full in the online Supplementary Material (Table S1, available at http://journals.cambridge.org/geo).

Three parameters are used to characterize the magnetic fabric: (1) the mean susceptibility, $k_m = (k_1 + k_2 + k_3)/3$, reflecting the magnetic mineral species and their proportion in the measured rock volume; (2) the degree of anisotropy, $P = k_1/k_3$, which expresses the eccentricity of the AMS ellipsoid; and (3) the shape parameter, $T = 2\ln(k_2/k_3)/\ln(k_1/k_3) - 1$, which describes the shape of the AMS ellipsoid; for $-1 \leq T < 0$ the ellipsoid is prolate, for $T = 0$ it is triaxial and for $0 > T \leq 1$ it is oblate. The maximum, intermediate and minimum susceptibility axes are k_1, k_2 and k_3, respectively. The maximum principal susceptibility (k_1) represents magnetic lineation and the minimum principal susceptibility (k_3) represents a pole to magnetic foliation. The orientation of magnetic foliations and lineations is plotted in the lower hemisphere stereograms and as the station mean directions on the map (calculated according to Jelínek, 1978).

5.b. Magnetic mineralogy

The mean (bulk) susceptibility of the vast majority (97 %) of specimens is in the order of 10^{-5} and 10^{-4} (SI units are used throughout this paper). Only 12 specimens have higher susceptibilities in the order of 10^{-3} (online Supplementary Figure S1, available at http://journals.cambridge.org/geo). Eight of the high-susceptibility specimens are from a single locality (MB42); the other four are scattered among different sites. The prevailing low susceptibilities therefore indicate that paramagnetic minerals control the AMS (e.g. Hrouda & Kahan, 1991) at all but one station. At station MB42, the AMS signal is dominated by ferromagnetic *sensu lato* minerals.

In order to confirm the paramagnetic or ferromagnetic mineralogy and to determine the AMS carriers, variation of the susceptibility to temperature was measured on four representative coarsely powdered specimens using the CS-L Cryostat and CS-4 Furnace instruments (Hrouda, 1994) in the Laboratory of Rock Magnetism, Institute of Geology and Palaeontology, Charles University in Prague. Specimens were heated from room temperature to *c.* 700 °C and cooled down to *c.* 40 °C at an approximate rate of 14 °C/min in argon atmosphere to minimize mineral changes due to oxidation. The data were statistically treated and plotted using the Cureval 8 software (Agico, Inc.). The thermomagnetic curves are

https://doi.org/10.1017/S0016756816000030 Published online by Cambridge University Press

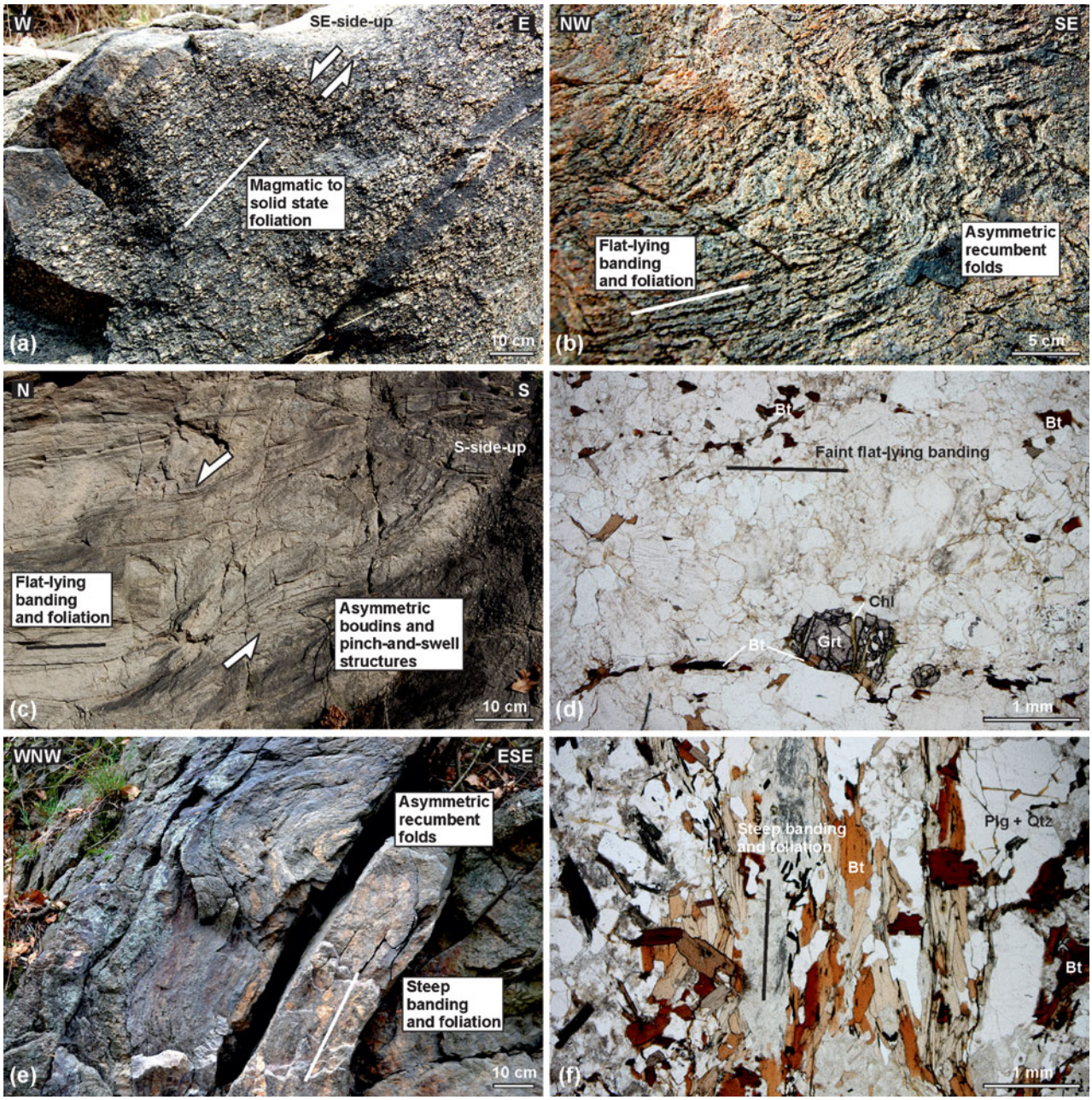

Figure 5. (Colour online) Examples of macroscopic fabrics, deformational microstructures and kinematic indicators in the NE inner part of the Podolsko complex. See Figure 2 for location of photographs. (a) Deformed melagranite with S–C fabric indicating normal, SE-side-up kinematics within the Červená shear zone. WGS84 coordinates: 49.33956° N, 14.28462° E. (b) Asymmetric, NW-vergent recumbent folds affecting flat-lying foliation in leucocratic migmatite. WGS84 coordinates: 49.33456° N, 14.29254° E. (c) Flat-lying foliation and banding in leucocratic migmatite affected by extensional shearing to form asymmetric boudins and pinch-and-swell structures indicating normal, S-side-up kinematics. WGS84 coordinates: 49.313101° N, 14.31687° E. (d) Photomicrograph of faint flat-lying banding in leucocratic migmatite. Microfractures in garnet porphyroclasts are filled by chlorite aggregates. Foliation perpendicular section, plane-polarized light. WGS84 coordinates: 49.33314° N, 14.29755° E. (e) Steep compositional banding and foliation in stromatic biotite migmatite of the Varied 'series' overprinted by asymmetric recumbent folds. WGS84 coordinates: 49.24155° N, 14.36235° E. (f) Photomicrograph of steep foliation and banding in stromatic biotite migmatite. Foliation perpendicular section, plane-polarized light. WGS84 coordinates: 49.29816° N, 14.34271° E.

provided in online Supplementary Figure S2 (available at http://journals.cambridge.org/geo).

Several types of thermomagnetic curves were obtained during the experiments. (1) The representative low-susceptibility specimens (leucocratic migmatite MB5/1/2 and stromatic biotite migmatite MB35/1/4 with $k_m = 4.93\times10^{-5}$ and 2.21×10^{-4}, respectively) show a gradual hyperbolic decrease in the bulk susceptibility across the measured temperature range. Such hyperbolic heating curves, where the magnetic susceptibility is inversely proportional to the absolute temperature according to the Curie–Weiss law, indicate paramagnetic minerals (biotite) as the dominant AMS carriers. For the latter specimen, a small bump on the otherwise hyperbolic curve at a temperature of *c.* 580 °C indicates a small admixture of magnetite. An additional

https://doi.org/10.1017/S0016756816000030 Published online by Cambridge University Press

Figure 6. (Colour online) Examples of macroscopic fabrics, deformational microstructures, and kinematic indicators in the mantling metasedimentary rocks to the E and SE of the Podolsko complex. See Figure 2 for location of photographs. (a) Irregular folds in strongly constricted paragneiss of the Varied 'series', lineation-perpendicular section. WGS84 coordinates: 49.24502° N, 14.39000° E. (b) Constrictional microfabric in paragneiss, lineation-perpendicular section, plane-polarized light. WGS84 coordinates: 49.24603° N, 14.39530° E. (c) Biotite paragneiss from an area north of the main Vodňany–Týn nad Vltavou shear zone but pervasively overprinted by SE-side-up normal shearing. WGS84 coordinates: 49.25438° N, 14.41937° E. (d) Photomicrograph of migmatitized paragneiss of the Varied 'series' affected by extensional microshears. Mica fish indicate normal, SE-side-up kinematics. WGS84 coordinates: 49.24682° N, 14.40687° E. (e) Pervasive foliation and asymmetric quartz boudins in mylonitized paragneiss of the Monotonous 'series' within the Vodňany–Týn nad Vltavou normal shear zone. WGS84 coordinates: 49.21252° N, 14.44059° E. (f) Photomicrograph of biotite–sillimanite paragneiss of the Monotonous 'series' with extensional crenulation cleavage indicating normal SSE-side-up kinematics of the Vodňany–Týn nad Vltavou normal shear zone. Lineation parallel and foliation perpendicular section, plane-polarized light. WGS84 coordinates: 49.21570° N, 14.43671° E.

increase on the cooling curves can be attributed to the growth of new magnetite as a result of decomposition and oxidation of Fe-bearing mineral phases with decreasing temperature. (2) The heating curve for an anomalous low-susceptibility but highly anisotropic and prolate specimen MB129/2/2 ($k_m = 7.28\times10^{-4}$, $P = 2.226$, $T = –0.211$) shows a decrease in its initial part, a pronounced peak at a temperature of *c.* 320 °C and then a near-hyperbolic decrease from that peak to the end of the temperature range. (3) The most complex heating curve was obtained for a high-susceptibility specimen MB42/3/1 ($k_m = 1.75\times10^{-3}$), which shows a nearly constant susceptibility in its initial part and then two pronounced peaks at temperatures of *c.* 300 °C and

https://doi.org/10.1017/S0016756816000030 Published online by Cambridge University Press

Table 1. Overview of U–Pb geochronology samples from the Podolsko complex (PC) and its metasedimentary mantling rocks (Varied 'series', VS).

Sample No.	Unit	Latitude (N), longitude (E) WGS84	Locality	Lithology
MB35	PC	49° 19' 58.4", 14° 17' 50.9"	Cliff on the left bank of the Vltava River, 80 m east of Svatý Jan	Weakly banded leucocratic garnet-bearing migmatite
MB126	VS	49° 14' 47.9", 14° 24' 27.0"	Cliff on the left bank of the Lužnice River, 1.8 km SE of Hosty	Stromatic biotite migmatite with sillimanite
MB144	PC	49° 21' 21.6', 14° 16' 48.6"	Flat outcrop in the Budovice Creek, 700 m SSE of Podolsko	Deformed granite with locally preserved magmatic texture
MB215	PC	49° 19' 18.1", 14° 11' 14.6"	Block from active quarry Brložnice, 3.5 km NE of Písek	Anatectic fine-grained equigranular biotite granite
JZ965	PC	49° 13' 47.0", 14° 14' 58.8"	Block from outcrop 250 m SW of Medenice	Retrogressed weakly banded felsic granulite

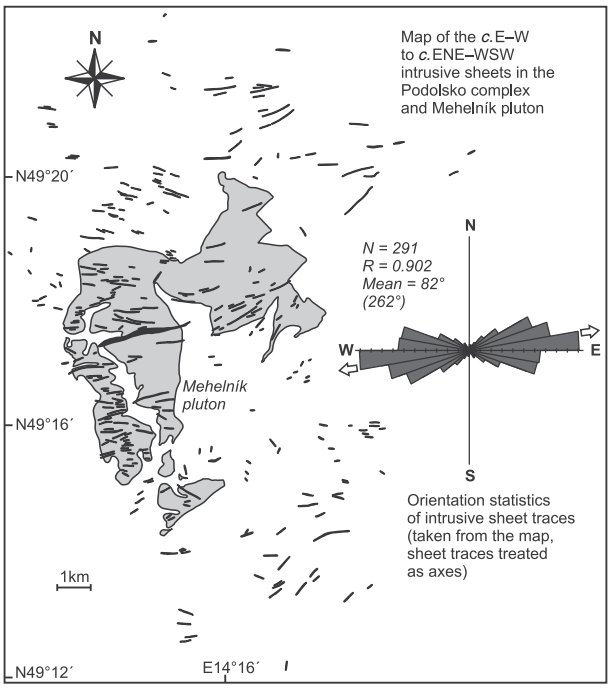

Figure 7. Simplified map highlighting *c.* E–W magmatic sheets cross-cutting the Podolsko complex and the melasyenite Mehelník pluton. The sheets exhibit a remarkably uniform orientation (inset rose diagram). Sheets were extracted from geological map in Figure 2.

520 °C. The latter two cases therefore indicate complex magnetic mineralogies and mixed contributions of biotite, pyrhotite and magnetite.

5.c. Magnetic fabric parameters and orientation

Together with the fairly uniform mineralogy, the degree of anisotropy is comparable in all sampled units and the *P* parameter mostly does not exceed 1.2 (corresponding to 20 % anisotropy), but is generally higher in the metasedimentary mantling rocks than in the Podolsko migmatites (online Supplementary Figure S1, available at http://journals.cambridge.org/geo). In both units, most of the AMS ellipsoids are oblate (78 % in the Podolsko complex, 70 % in the mantling rocks), with a slight tendency of an increasing degree of oblateness with an increasing degree of anisotropy. The exceptions to the above are the pyrhotite-bearing specimens from station MB42 (leucocratic migmatite), with *P* between 1.016 and 1.551, and specimens from station MB129 (stromatic biotite migmatite) with prolate AMS ellipsoids and *P* as high as 2.321.

At most stations, the measured orientations of the principal susceptibility axes are clustered, the site-mean directions are well defined and the mean magnetic foliation corresponds well to the metamorphic foliation and compositional banding. In Domain 1, magnetic foliations dip at low to moderate angles and have variable strikes, whereas in Domain 2 they strike roughly N–S and dip moderately in most cases (Fig. 8). In most of Domain 3, foliations dip steeply to moderately to the *c.* SW, but in its southern portion scatter along a *c.* N–S direction or become subparallel to the Vodňany–Týn nad Vltavou shear zone at the two southernmost stations (Fig. 8). The most striking feature of magnetic fabric in the Podolsko complex and its mantling rocks is, however, that magnetic lineations plunge shallowly to the *c.* N–NNW or to the *c.* S–SSE across the different structural domains regardless of lithology, degree of anatexis or location (Fig. 8). Magnetic lineations therefore exhibit a clustered orientation distribution on the stereonet, whereas magnetic foliation poles define a girdle about the mean magnetic lineation of 336°/04° (Fig. 8; calculated from all specimens using the method of Jelínek, 1978, 1981).

6. U–Pb zircon geochronology

6.a. Analytical methods

Five samples of *c.* 30–40 kg each were taken along an approximately N–S-oriented transect across the complex and at one locality off this transect (see Fig. 2 for sample locations). The sampling strategy was to cover the main rock types of the Podolsko complex and the mantling migmatites of the Varied 'series'. Sample descriptions are given in Table 1. The samples were then crushed, the zircon grains separated using the Wilfley shaking table and heavy liquids in the laboratories of the Czech Geological Survey, Prague, and finally mounted in epoxy-filled blocks and polished for subsequent cathodoluminescence (CL) imaging.

https://doi.org/10.1017/S0016756816000030 Published online by Cambridge University Press

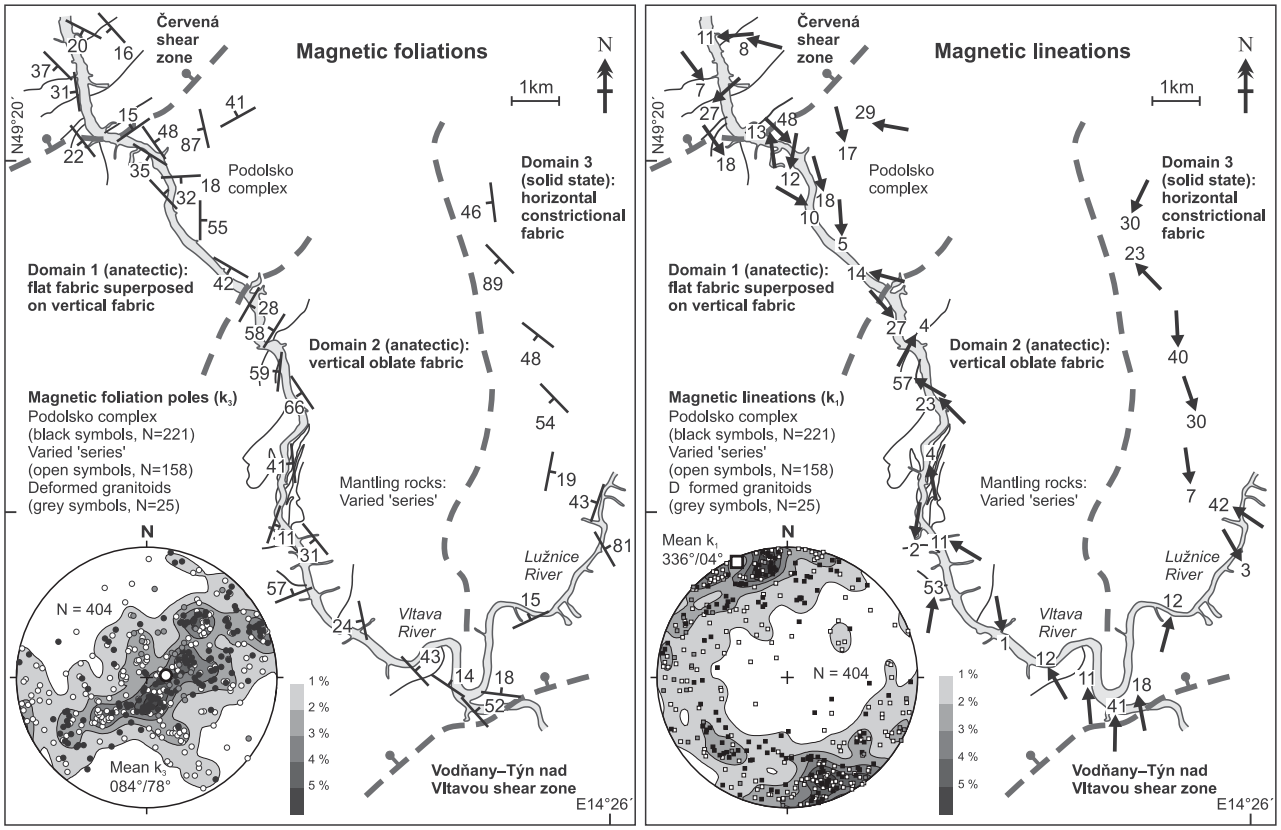

Figure 8. Maps showing orientations of magnetic foliations and lineations in the Podolsko complex and its mantling rocks. Stereonets (equal area, lower-hemisphere projections) summarize orientation of magnetic foliations and lineations.

The Nu AttoM high-resolution ICP-MS coupled to a 193 nm ArF excimer laser (Resonetics RESOlution M-50 LR) at Bergen University, Norway, was used to measure the Pb/U and Pb isotopic ratios in zircons over the course of three individual analytical sessions. The laser was fired at a repetition rate of 4 Hz and energy of 80 mJ with 19 microns spot size. Typical acquisition consisted of a 15 s measurement of blank, followed by a measurement of U and Pb signals from the ablated zircon for another 30 s. The data were acquired in time-resolved peak-jumping pulse-counting mode with one point measured per peak for masses ^{204}Pb + Hg, ^{206}Pb, ^{207}Pb, ^{208}Pb, ^{232}Th, ^{235}U and ^{238}U. Due to a non-linear transition between the counting and attenuated (= analogue) acquisition modes of the ICP instruments, the raw data were pre-processed using a purpose-made Excel macro. As a result, the intensities of ^{238}U are left unchanged if measured in a counting mode and recalculated from ^{235}U intensities if the ^{238}U was acquired in an attenuated mode. Data reduction was then carried out off-line using the Iolite data reduction package version 3.0 with VizualAge utility (Petrus & Kamber, 2012). Full details of the data reduction methodology can be found in Paton *et al.* (2010). It included correction for gas blank, laser-induced elemental fractionation of Pb and U and instrument mass bias. For the data presented here, blank intensities and instrumental bias were interpolated using an automatic spline function while down-hole inter-element fractionation was corrected using an exponential function. No common Pb correction was applied to the data, but the low concentrations of common Pb were controlled by observing the ^{206}Pb/^{204}Pb ratio during measurements. Residual elemental fractionation and instrumental mass bias were corrected by normalization to the natural zircon reference material GJ-1 (Jackson *et al.* 2004). Plešovice (Sláma *et al.* 2008) and 91500 (Wiedenbeck *et al.* 1995) zircon reference materials were periodically analysed during the measurement for quality control and the obtained mean values of 339.6 ± 0.7(2σ) Ma and 1066 ± 2(2σ) Ma are 1 % accurate within the published reference values (337 Ma, Sláma *et al.* 2008; 1065 Ma, Wiedenbeck *et al.* 1995). The zircon U–Pb ages are presented as concordia diagrams and probability density plots, generated with the ISOPLOT program v. 3.50 (Ludwig, 2008).

The measured U–Pb zircon data and cathodoluminescence (CL) images are presented in Figures 9–18 and listed in full in the online Supplementary Table S2 (available at http://journals.cambridge.org/geo).

6.b. Results: zircon U–Pb data

6.b.1. Sample MB35 (leucocratic migmatite)

The sample contains mostly euhedral, long prismatic zircon grains with well-preserved faces (Fig. 10). Some grains are clear, but a large proportion of brown-coloured crystals point to pronounced metamictization and lead loss affecting the zircon. The inner textures of

https://doi.org/10.1017/S0016756816000030 Published online by Cambridge University Press

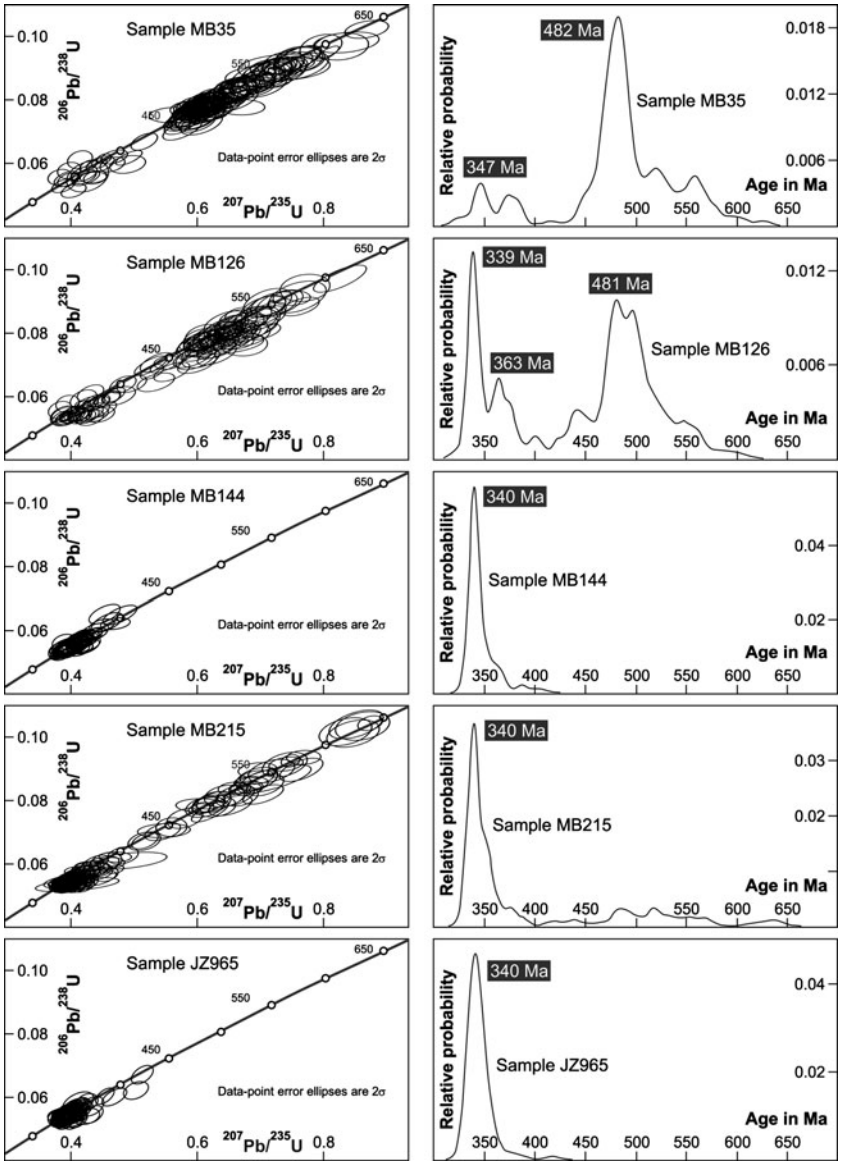

Figure 9. Concordia diagrams and zircon age spectra (probability density plots) of the analysed samples from the Podolsko leucocratic migmatite (sample MB35), biotite migmatite of the Varied 'series' (sample MB126), deformed granite (sample MB144), anatectic granite (sample MB215) and retrogressed granulite (sample JZ965).

polished zircon grains together with U–Pb data reveal various degrees of isotopic disturbance and the presence of older cores enclosed within younger growth zones (Fig. 10). There are only a few zircon grains with ages older than *c.* 700 Ma. The majority of the data plot along the concordia over the range *c.* 630–340 Ma (Fig. 9), with the highest density at *c.* 480 Ma. The mean age of 482 ± 1.7 Ma (Figs 9, 15), obtained from the euhedral prismatic grains with medium-CL intensity, probably records the event of magmatic zircon growth. The zircons with near-concordant or slightly discordant ages between *c.* 630 Ma and *c.* 482 Ma represent the inherited zircon component. They occur either as individual crystals (xenocrysts) or as partially resorbed cores overgrown by younger, *c.* 482 Ma old zircon (Fig. 10). Some of these inherited zircons were subjected to partial lead loss during the *c.* 482 Ma thermal event. The few discordant ages younger than 482 Ma show a trend towards *c.* 340 Ma but the absence of a clear age cluster suggests that this was only a lead loss event with limited or no growth of new zircon. The presence of a single zircon grain with oscillatory zoning, medium-CL intensity and concordant age of *c.* 340 Ma cannot be taken as evidence of new zircon formation. The *c.* 340 Ma event affected mostly the CL-dark, U-rich zircon grains (Fig. 10), which are known to be prone to lead loss during protracted thermal overprint. One of the metamict zircon grains shows a complete reset of U–Pb to *c.* 340 Ma (Fig. 10).

6.b.2. Sample MB126 (migmatitized paragneiss)

In terms of the obtained ages, this sample is similar to sample MB35. With the exception of two older zircon ages of *c.* 2.2 and *c.* 2.1 Ga, all the data plot within the range *c.* 610–340 Ma (Fig. 9). The visual

https://doi.org/10.1017/S0016756816000030 Published online by Cambridge University Press

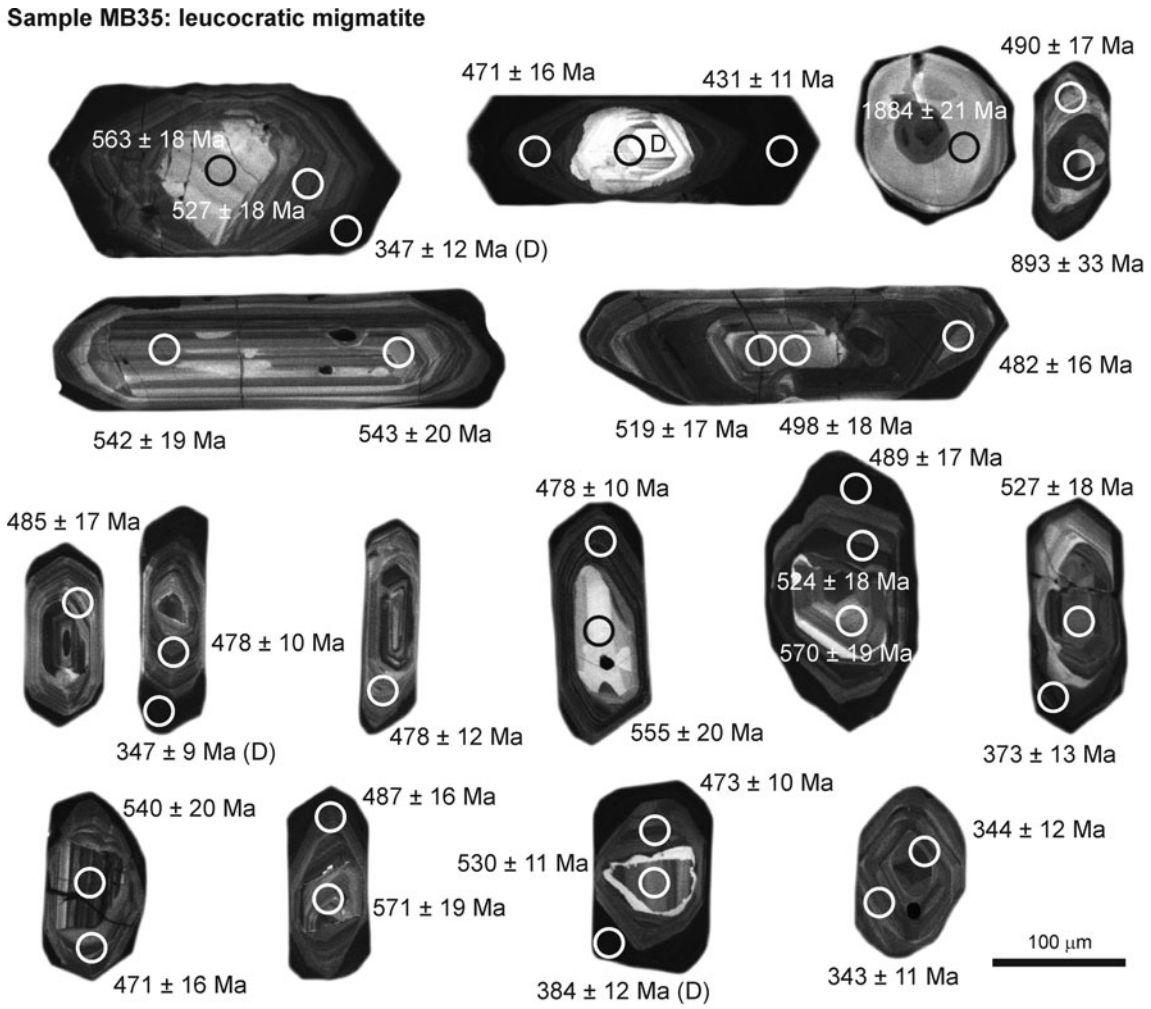

Figure 10. Representative cathodoluminescence images of zircon from sample MB35. The spots where laser-ablation analysis was performed are indicated together with the obtained $^{206}Pb/^{238}U$ ages. D – discordant analysis.

inspection of zircon under binocular microscope and CL imaging revealed a higher degree of metamictization with a darker appearance of the investigated grains (Fig. 11). The U–Pb data show a higher abundance of *c.* 340 Ma ages with respect to *c.* 480 Ma mode in the probability density plot, when compared to sample MB35 (Fig. 9). There are fewer prismatic zircon grains with medium-CL intensity than in sample MB35 (Fig. 11b). However, their mean U–Pb age of 480.6 ± 3.7 Ma (Fig. 16a) is identical within the analytical uncertainty to those in the sample MB35. We consider this age to represent the growth of magmatic zircon during the proto-source melting. Despite their higher discordance, the ages that cluster at *c.* 480 Ma represent the most abundant zircon component in the sample.

The higher abundance of *c.* 340 Ma ages suggests that the lead loss event had a larger impact on sample MB126 as compared to sample MB35 (Figs 9, 16b). On the other hand, this could merely be an effect of a higher content of U in the original zircon grains of MB126 and hence stronger metamictization of zircon lattice prior to *c.* 340 Ma. Besides a group of zircons with intermediate U–Pb ages between *c.* 480 and 340 Ma, there is also a distinct cluster of completely reset U-rich zircons (Fig. 11c) with a mean age of 338.5 ± 2.2 Ma (Fig. 16b). None of the analysed zircons appear to have grown at *c.* 340 Ma.

6.b.3. Sample MB144 (deformed granite)

The lack of variation in appearance of zircon grains in sample MB144 corresponds to the still well-preserved magmatic texture of the granite (Fig. 12). Cathodoluminescence imaging revealed two distinct populations of zircon crystals: (1) euhedral prismatic zircons with simple pyramid terminations and dark-CL intensities, which make up a relatively small proportion of the bulk zircon content (Fig. 12a); and (2) stubby crystals with a complex pyramid termination, typical oscillatory zonation and medium-CL intensity, which account for most of the analysed zircon grains (Fig. 12b). The U–Pb data of the CL-dark population spread between *c.* 400–340 Ma, indicating that it represents an older, probably inherited zircon population with lead loss towards *c.* 340 Ma (Fig. 12). The youngest and completely reset zircons of this population make up a cluster with a U–Pb mean age of 340.5 ± 4.5 Ma (Figs 9, 16c). The

https://doi.org/10.1017/S0016756816000030 Published online by Cambridge University Press

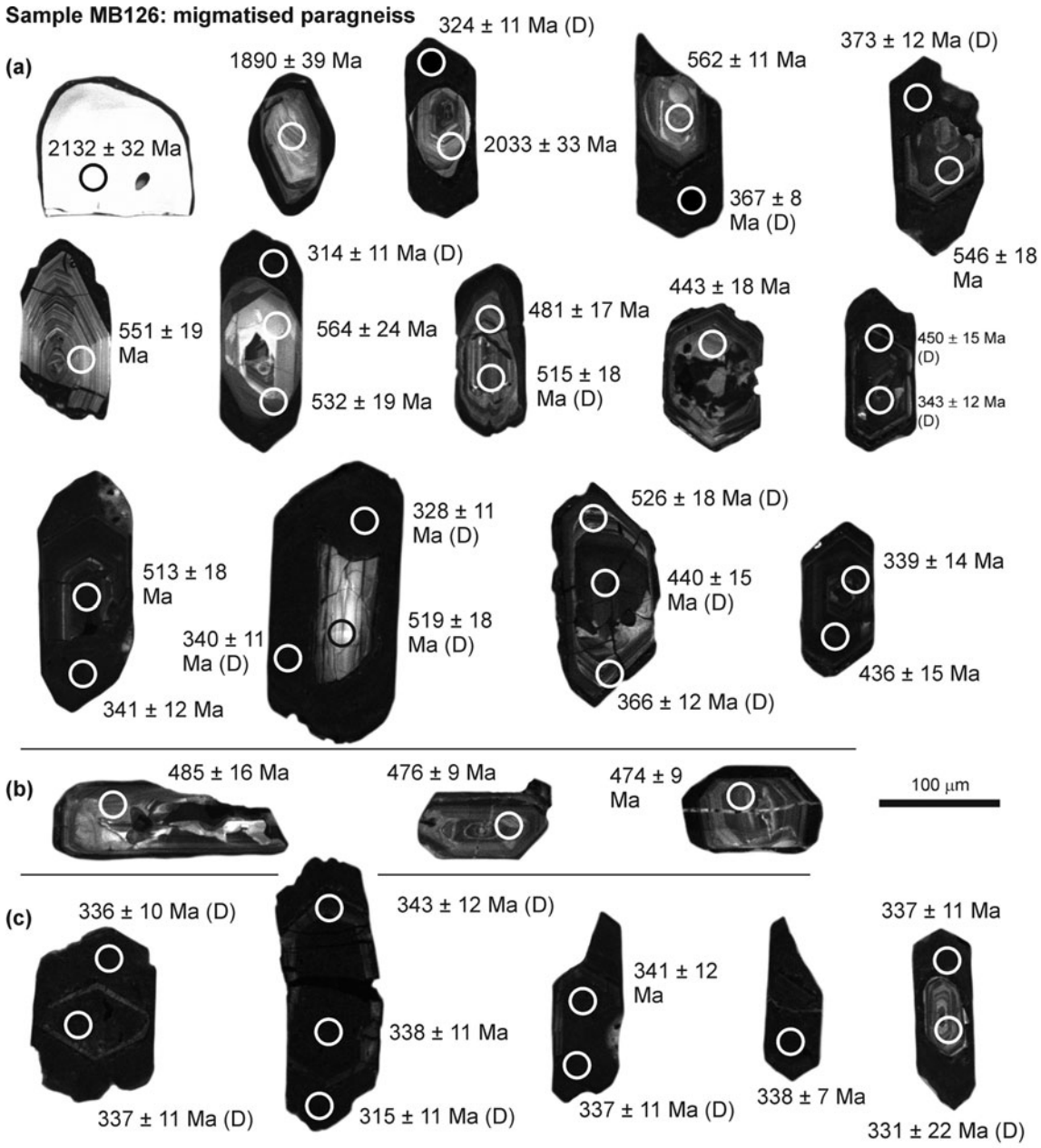

Figure 11. Representative cathodoluminescence images of zircon from sample MB126. The spots where laser-ablation analysis was performed are indicated together with the obtained $^{206}Pb/^{238}U$ ages. D – discordant analysis.

dating of zircon population (2) with typical magmatic textures provided a mean age of 339.8 ± 1.0 Ma (Fig. 16d) which is identical, within analytical uncertainty, to the age of the completely reset inherited population. The data provide evidence of a magmatic event at *c.* 340 Ma, with the growth of new zircon as well as thermally induced lead loss of the older metamictized zircon xenocrysts. The limited number of inherited zircon grains and their strong isotopic disturbance preclude assessment of the nature and age of the sample MB144 precursor.

6.b.4. Sample MB215 (anatectic granite)

This sample contains a few zircons with ages of *c.* 2.6, 2.5, 2.0, 1.8, 0.9 and 0.7 Ma (Fig. 9). The grains with ages older than *c.* 500 Ma occur either as xenocrysts or as resorbed residues preserved as cores overgrown by younger zircon (Fig. 13a). The *c.* 480 Ma peak found in samples MB35 and MB126 is missing in sample MB215 (Fig. 9). This age is only represented by a few prismatic grains with a typical magmatic zonation and medium-CL intensities (Fig. 13c). The sample records a significant event at *c.* 340 Ma, as shown in the probability density plot. The careful examination of CL images (Fig. 13) and U–Pb data (Figs 9, 17) unveiled three different mechanisms that have probably led to the formation of zircon with *c.* 340 Ma age.

(1) A large proportion of zircon grains with dark-CL intensities and convoluted or featureless textures plots along concordia over the range *c.* 390–340 Ma and is most probably the product of the isotopic reset

https://doi.org/10.1017/S0016756816000030 Published online by Cambridge University Press

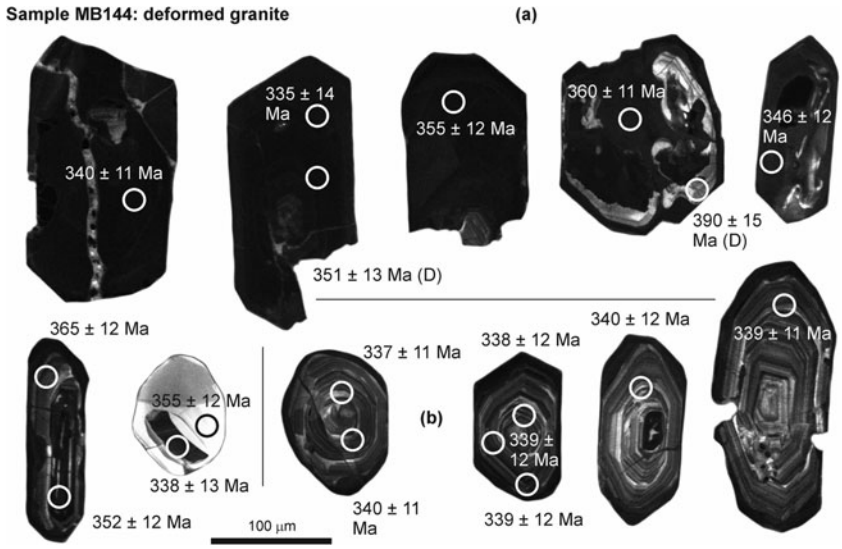

Figure 12. Representative cathodoluminescence images of zircon from sample MB144. The spots where laser-ablation analysis was performed are indicated together with the obtained $^{206}Pb/^{238}U$ ages. D – discordant analysis.

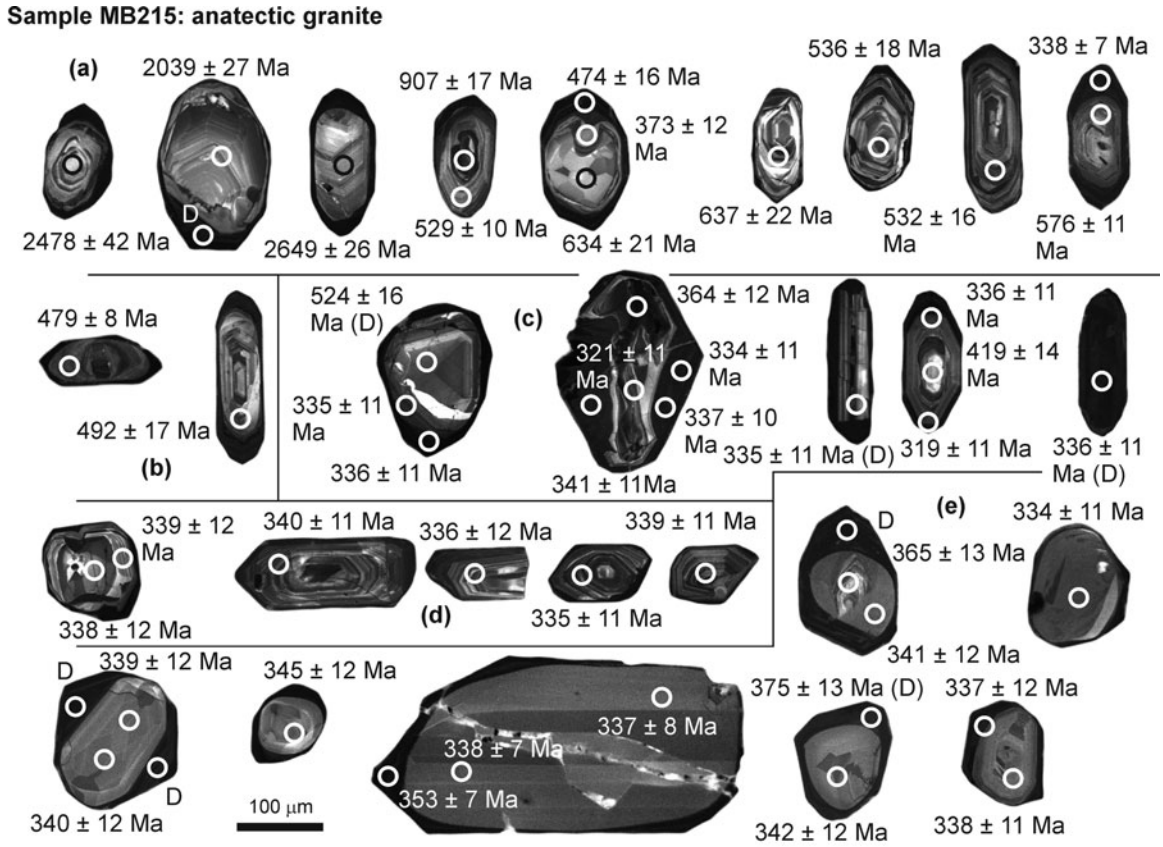

Figure 13. Representative cathodoluminescence images of zircon from sample MB215. The spots where laser-ablation analysis was performed are indicated together with the obtained $^{206}Pb/^{238}U$ ages. D – discordant analysis.

(= lead loss) of older zircon grains. They have a high U content (an average of 1370 ppm). The youngest concordant ages provide a mean age of 340 ± 1.7 Ma (Figs 13c, 17b).

(2) Several zircon grains form euhedral, prismatic to stubby crystals with well-shaped faces and typical magmatic inner textures with oscillatory zonation of medium-CL intensities (Fig. 13d) and average U content of 529 ppm. All the U–Pb data obtained from these grains form a cluster with a mean age of 339.7 ± 2.2 Ma (Fig. 17c).

(3) Some zircon grains show a unique texture where an inner part of elliptical shape, medium-CL intensity and sector zonation is enclosed by a CL-dark rim with faded relics of probably oscillatory zonation (Fig. 13e). The dark rims have high U

https://doi.org/10.1017/S0016756816000030 Published online by Cambridge University Press

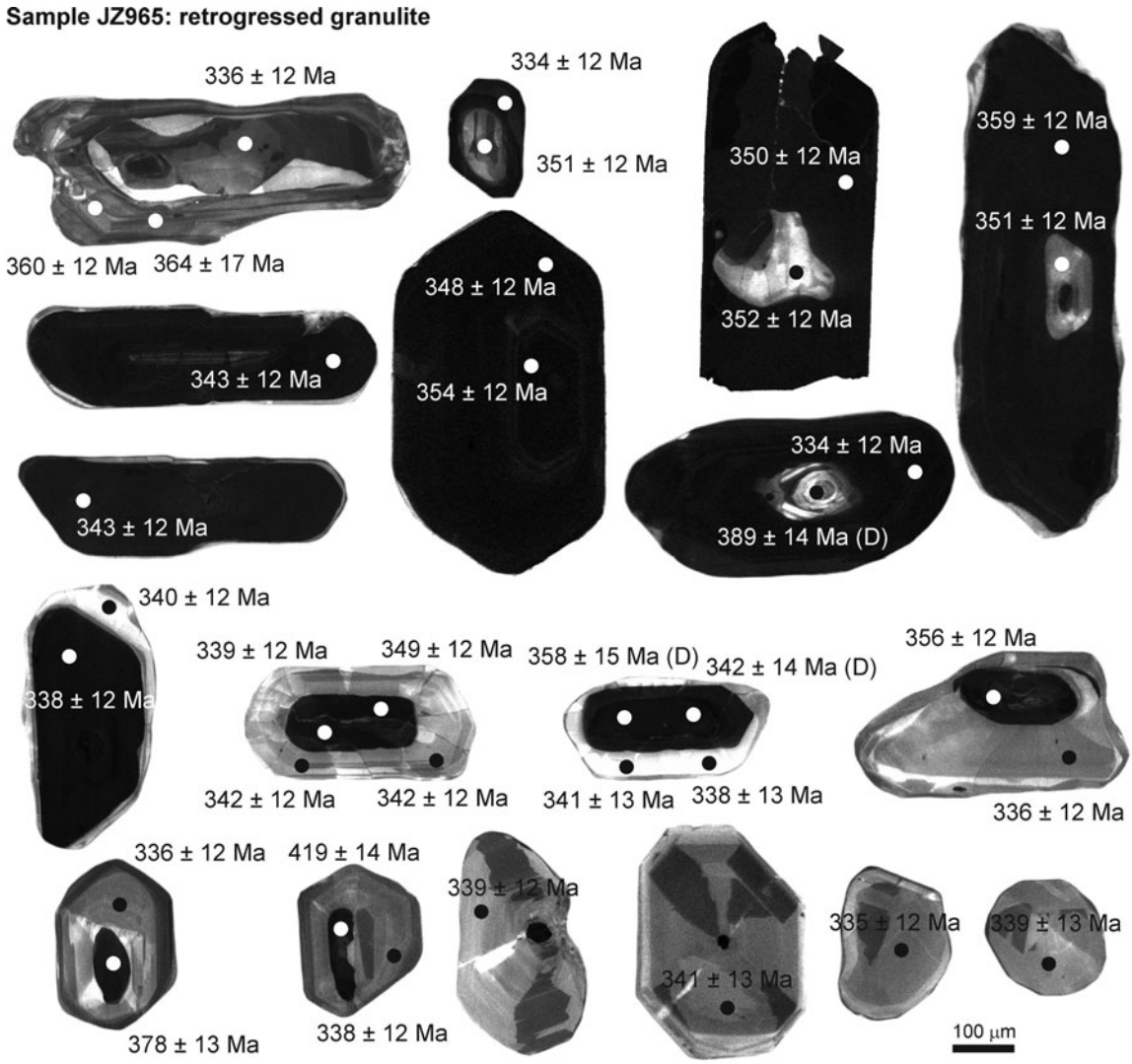

Figure 14. Representative cathodoluminescence images of zircon from sample JZ965. The spots where laser-ablation analysis was performed are indicated together with the obtained $^{206}Pb/^{238}U$ ages. D – denotes discordant analysis.

concentrations (an average of 2144 ppm) and a variable content of Pb (5–7529 ppm, an average of 2614 ppm), corresponding to their supposed strong lattice damage (metamictization). Their U–Pb age data are strongly discordant with a few analyses between *c.* 375 and *c.* 337 Ma, documenting U–Pb reset towards the younger age. The inner parts show textures that are typical for zircons crystallized at a high metamorphic grade. They have normal contents of both U (average of 395 ppm) and Pb (average of 37 ppm) and the U–Pb dating provided a mean age of 340.8 ± 1.4 Ma (Fig. 17d).

The three different types of zircon with ages of *c.* 340 Ma detected in the sample record a significant tectono-metamorphic event that probably included remelting of the source rock, facilitating crystallization of new magmatic zircon grains. The elevated temperatures also triggered U–Pb age reset (= lead loss) and new growth of zircon in U-rich metamict zircons. The appearance of the newly grown metamorphic zircons suggests that the rock might have undergone incipient granulite-facies metamorphism.

6.b.5. Sample JZ965 (felsic granulite)

Two types of zircon were identified in sample JZ965. The first type is represented by large prismatic grains, almost featureless and dark in CL (Fig. 14) and with a high content of U (average of 1664 ppm). The crystal faces are usually uneven with signs of recrystallization and resorption. Relics of CL-bright inner parts are preserved in some of these grains (Fig. 14). The U–Pb data fell within the range *c.* 420–340 Ma, suggesting they are older zircons with partial to complete lead loss at *c.* 340 Ma. The youngest cluster of ages provides a mean age of 339.1 ± 1.5 Ma (Fig. 18a). One grain with a lower U content (375 ppm) and medium-CL intensity (first grain in Fig. 14) shows slightly discordant ages of *c.* 360 Ma in the outer part and *c.* 336 Ma age in the inner, probably fully annealed part. The second type represents the typical granulite-facies zircons with stubby and soccer-ball habits and sector zonation textures in CL (Fig. 14). This type commonly overgrows the older CL-dark zircon. It documents new zircon growth at granulite-facies conditions with a mean age

https://doi.org/10.1017/S0016756816000030 Published online by Cambridge University Press

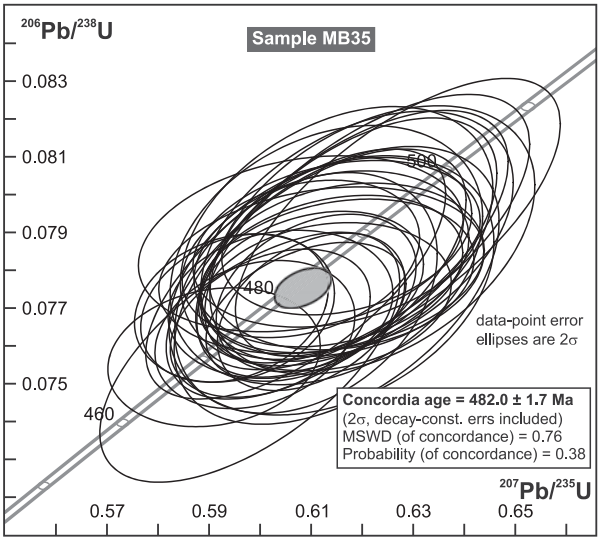

Figure 15. Concordia diagram for sample MB35 with a zircon weighted mean (concordia) Pb/U age.

of 339.6 ± 1.2 Ma (Fig. 18b). The JZ965 sample contains on average much larger zircon grains (typically 300–800 μm) than the other studied samples, which suggests a different protolith.

7. Discussion

7.a. Chronology of events recorded in the Podolsko complex and its mantling rocks

Despite the pre-Variscan tectonic history of the Podolsko complex having been largely masked by the pervasive anatexis, our geochronologic data point to an Early Ordovician (*c.* 480 Ma) age of igneous protolith of the granulites and leucocratic migmatites and melting of the proto-source of the metapelitic migmatites of the Varied 'series' (Figs 9, 15, 16a). These findings are in agreement with what is well known from elsewhere in the Saxothuringian, Teplá–Barrandian and Moldanubian units and corroborate that the Cadomian basement in much of the Bohemian Massif underwent a widespread Cambro–Ordovician rifting and related LP–HT anatexis, plutonism and basin development (Fig. 19a; e.g. Kachlík & Patočka, 1998; Crowley *et al.* 2000; Dostal, Patočka & Pin, 2001; Pin *et al.* 2007; Žák, Kraft & Hajná, 2013). The early Variscan (Middle–Late Devonian) history of the Podolsko complex is difficult to reconstruct due to the gap in the rock record. Nevertheless, the presence of HP–UHP garnetites (Kotková, Harley & Fišera, 1997) and the newly discovered relic prograde garnet zoning in the mafic granulites (Faryad & Žák, 2016) suggest that at least some portions of the complex witnessed subduction to mantle depths and low-temperature eclogite-facies metamorphism prior to the extensive anatexis in the middle crust (Fig. 19a). Most of our new U–Pb ages reflect this latter event and indicate wholesale thermally induced isotopic resetting and new crystallization of zircons at *c.* 340–339 Ma (Figs 9, 15, 17, 18). The deformed granite (sample MB144), previously mapped as an 'orthogneiss', has virtually the same magmatic crystallization age of *c.* 340 Ma (Figs 12, 16c, d) and is interpreted here as a syntectonic intrusion. Field relations together with the high-precision U–Pb ages therefore indicate a rather narrow time span of the high-temperature anatexis and coeval ductile deformation of the Podolsko complex and its mantling rocks between *c.* 340 Ma and *c.* 338–337 Ma. The latter age bracket is provided by a discordant pluton and dykes cross-cutting the ductile fabric along the southern margin of the Central Bohemian Plutonic Complex (Žák, Holub & Verner, 2005; Holub, Verner & Schmitz, 2011).

7.b. Tectonic reinterpretation of the Podolsko complex

The structural data presented above suggest that the Podolsko complex and its metasedimentary mantling rocks underwent an early *c.* E–W horizontal shortening, followed by a switch in the principal strain axes to dominant vertical shortening (Figs 3, 19b). Importantly, the subhorizontal *c.* NNW–ESE magnetic lineations are homogeneously oriented across the entire area and are nearly perpendicular to the late *c.* E–W dykes (Figs 7, 8). Regardless of whether the lineations represent elongation or the zone axis of biotite aggregates (e.g. Henry, 1997; Kruckenberg *et al.* 2010), they imply a single principal stretching direction during both deformations (Fig. 19b) which continued after cooling into the brittle regime. Virtually the same principal stretching direction was inferred for the deformed *c.* 346 Ma upper-crustal granitoids north of the Podolsko complex (Žák *et al.* 2012). The roughly E–W gradient in the degree of anatexis (Fig. 2), together with the fabric patterns being smoothly continuous across these domains (Fig. 3), suggests a transition from melt-present to solid-state ductile flow in the direction away from the anatectic core of the complex. The presence or absence of melt during deformation most probably controlled the extensive reworking or preservation of early steep fabrics in the anatectic core and in solid-state mantling rocks, respectively, and therefore also variations in the strain symmetry from oblate to constrictional.

The almost identical U–Pb ages (*c.* 340–339 Ma), similar metamorphic grade during the widespread anatexis and an inferred single principal stretching direction indicate that the steep and flat-lying fabrics do not represent two separate deformation phases; rather, they formed in a kinematic continuum during exhumation and cooling of the whole complex (Fig. 19b). This interpretation is in agreement with recent numerical models of dome growth in metamorphic core complexes. For instance, Rey *et al.* (2011) and Roger *et al.* (2015) documented a progressive transition from vertical fabric resulting from convergent viscous flow of partially molten crust at deeper levels to horizontal fabric resulting from extension in the upper crust. We therefore suggest that the Podolsko complex, with high-pressure rocks already included (mechanisms of their initial exhumation remain unknown), was upwelled within the

https://doi.org/10.1017/S0016756816000030 Published online by Cambridge University Press

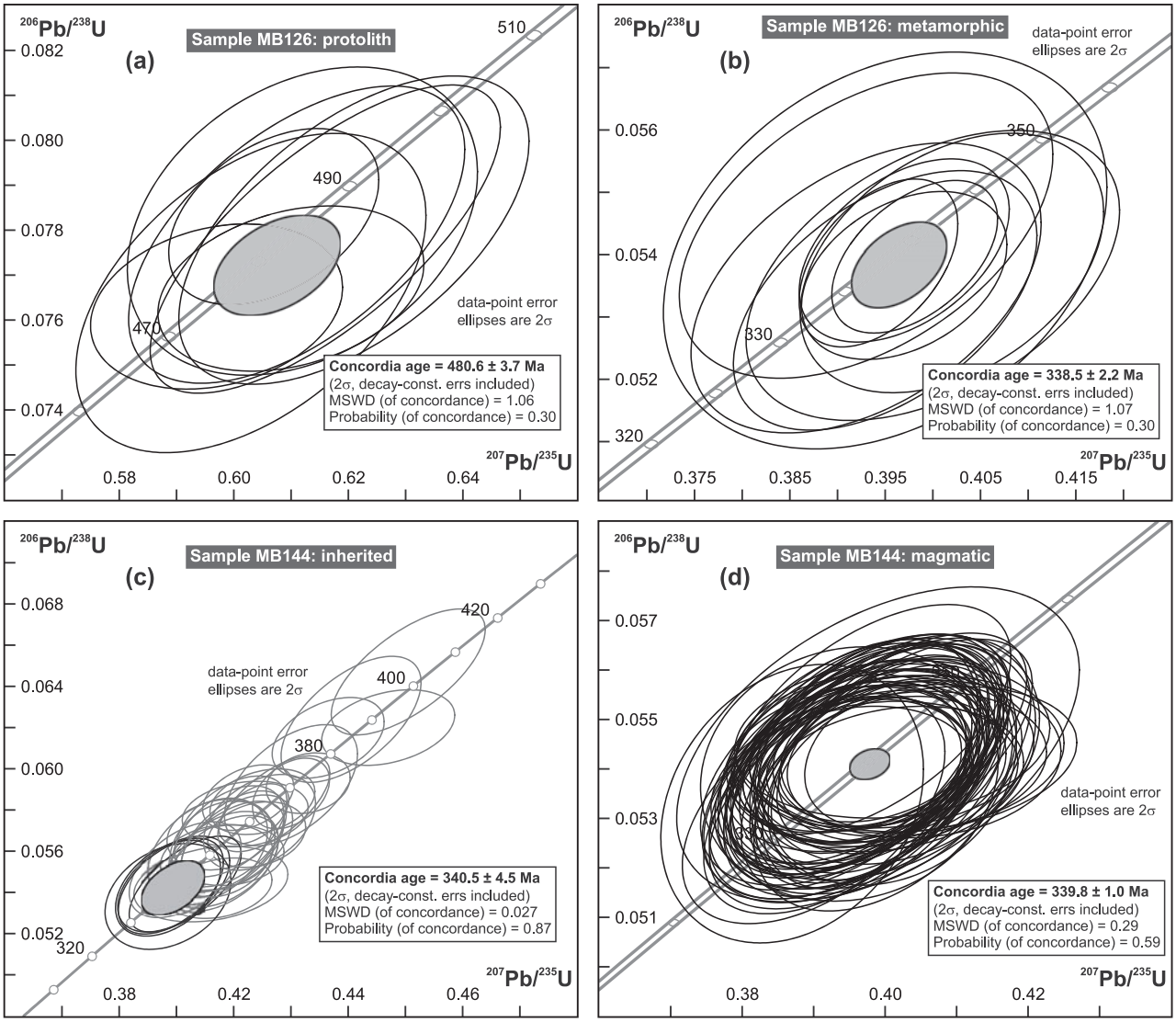

Figure 16. Concordia diagrams for samples (a, b) MB126 and (c, d) MB144 with zircon weighted mean (concordia) Pb/U ages. The grey ellipses in (c) were not included in the calculation of the respective concordia age.

ductile middle crust during lateral *c.* E–W shortening and *c.* NNW–SSE stretching to form an asymmetric domal structure with a hot migmatite–granite core and colder mantling sediments preserved on both sides (Fig. 19b). This process was perhaps driven by a combination of buoyancy, assuming that partially molten metapelitic and felsic rocks will be buoyant, and lateral tectonic forces, as evidenced by the steep foliation and horizontal magnetic lineations. Soon after, the whole dome collapsed vertically and its further exhumation was taken over by the more localized crustal-scale extensional detachments, the movements along which continued under the greenschist facies conditions. The detachments cut the dome at a high angle to the previous *c.* N–S structural grain but still accommodated the same *c.* NNW–SSE principal stretching (Figs 7, 8, 19b).

In summary, the observed widespread anatexis in the Podolsko complex is compatible with rapid exhumation of hot material to shallow levels, accommodated by fast extension strain rates in the upper crust (Rey, Teyssier & Whitney, 2009*a*, *b*). It also seems likely that the far-field orogen-parallel stretching of the upper crust may have been a key process driving formation of the Podolsko dome (e.g. Brun & Van Den Driessche, 1994; Tirel, Brun & Burov, 2004; Rey, Teyssier & Whitney, 2009*a*, *b*; Roger *et al.* 2015; Whitney *et al.* 2015).

The interpretations developed above challenge the long-held view of the Podolsko complex as part of the extensive SE-directed Gföhl nappe rooted along the Teplá–Barrandian/Moldanubian boundary and transported over non-anatectic, lower-grade metasedimentary rocks (the Varied and Monotonous 'series') across much of the Moldanubian unit (e.g. Tollmann, 1982; Franke, 2000, 2006). Instead, we suggest that it formed as an asymmetric granite–migmatite dome in the footwall of a major detachment (the Červená shear zone) separating the upper crust from the deep-crustal interior of the orogen. Another subparallel detachment (the Vodňany–Týn nad Vltavou shear zone) truncates the southern margin of the Podolsko complex and, as opposed to the previous poorly supported thrust-fault

https://doi.org/10.1017/S0016756816000030 Published online by Cambridge University Press

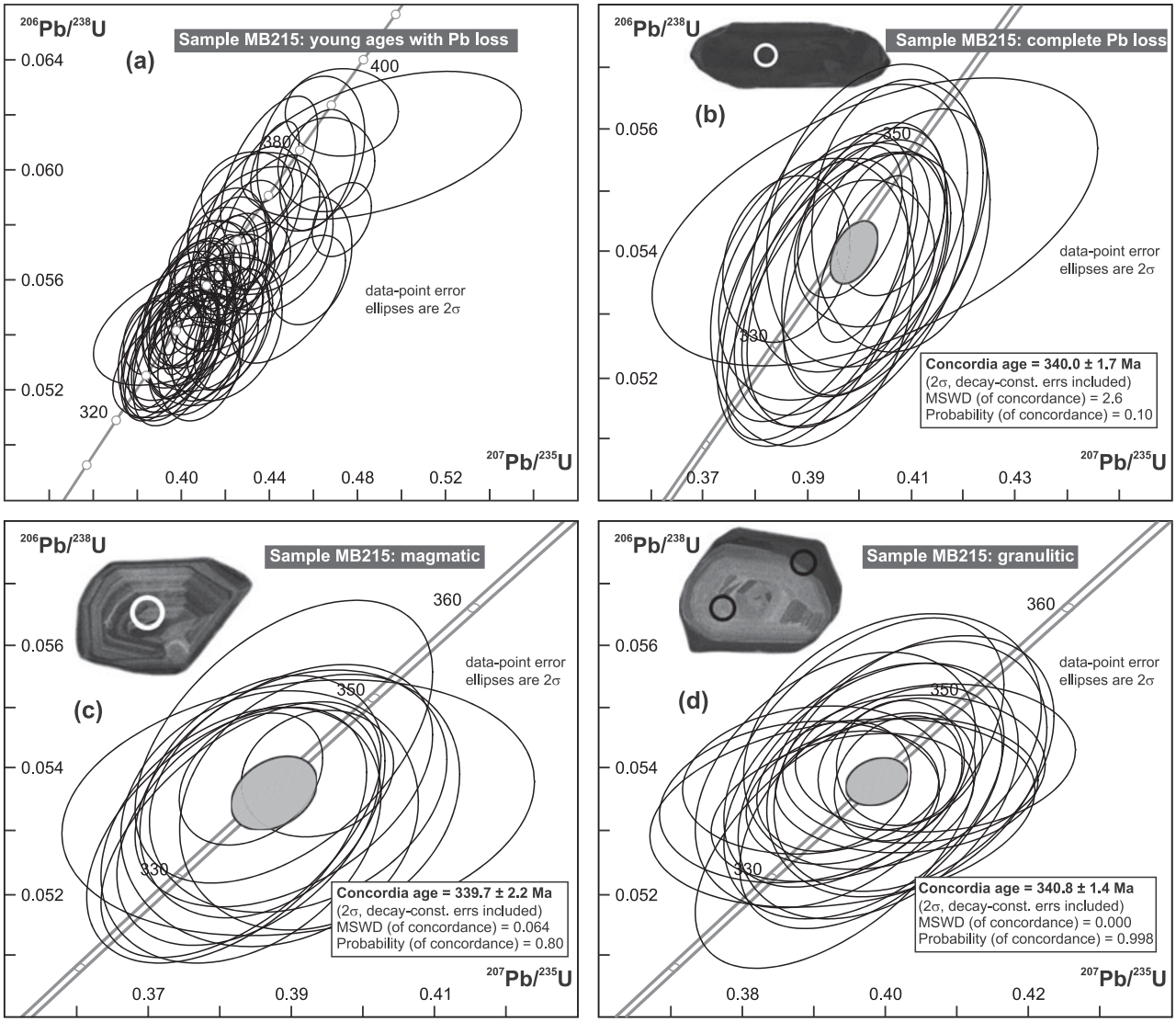

Figure 17. Concordia diagrams for sample MB215 with zircon weighted mean (concordia) Pb/U ages.

interpretation of Vrána (1979, 1988), is also interpreted here to record normal kinematics and the same crustal extension (Figs 3, 4, 6c, d, 19b).

7.c. The significance and geodynamic causes of the Variscan *c.* 340 Ma event

The *c.* 340 Ma U–Pb ages detected in the Podolsko complex and its mantling rocks are almost identical within analytical uncertainties to a number of ages reported from some eclogites (e.g. Brueckner, Medaris & Bakun-Czubaróv, 1991; Beard *et al.* 1992; Medaris *et al.* 1995), high-pressure granulites (overviews in Kröner *et al.* 2000; Janoušek & Holub, 2007 and Kotková, 2007) and ultrapotassic plutons (e.g. Holub, Cocherie & Rossi, 1997; Janoušek & Holub, 2007; Kotková, Schaltegger & Leichmann, 2010; Kusiak *et al.* 2010) scattered within the Moldanubian unit and from a gabbro–peridotite intrusive complex at its NE margin (Ackerman, Pašava & Erban, 2013). On a continental scale, the *c.* 340 Ma ages have also been reported from other units along the Variscan orogenic belt in central and western Europe, including Saxothuringian and Eger Complex granulites (e.g. Kotková *et al.* 1995; Kröner *et al.* 1998; Romer & Rötzler, 2001; Konopásek *et al.* 2014), mafic to felsic granitoid plutons in Odenwald (Altherr *et al.* 1999), K–Mg plutons in the Vosges Mountains (Schaltegger *et al.* 1996; Skrzypek, Štípská & Cocherie, 2012; Tabaud *et al.* 2014) and Variscan basement massifs of the Alps (Rubatto *et al.* 2010; von Raumer *et al.* 2013) and Corsica (Giacomini *et al.* 2008). In particular, the widespread *c.* 340–335 Ma durbachite–vaugnerite suite was used as an argument for a short-lived but orogen-wide thermal pulse (von Raumer *et al.* 2014).

While most studies agree that the *c.* 340 Ma tectonothermal event must have represented a milestone in the evolution of the Variscan orogenic belt, significant controversies persist regarding its geodynamic causes. In the Bohemian Massif, the unresolved major issues include: (1) the palaeogeographic setting and the location and polarity of oceanic and continental subductions at that time (e.g. Franke, 2000, 2006; Medaris *et al.* 2005; Finger *et al.* 2007; Schulmann *et al.* 2009*b*, 2014;

https://doi.org/10.1017/S0016756816000030 Published online by Cambridge University Press

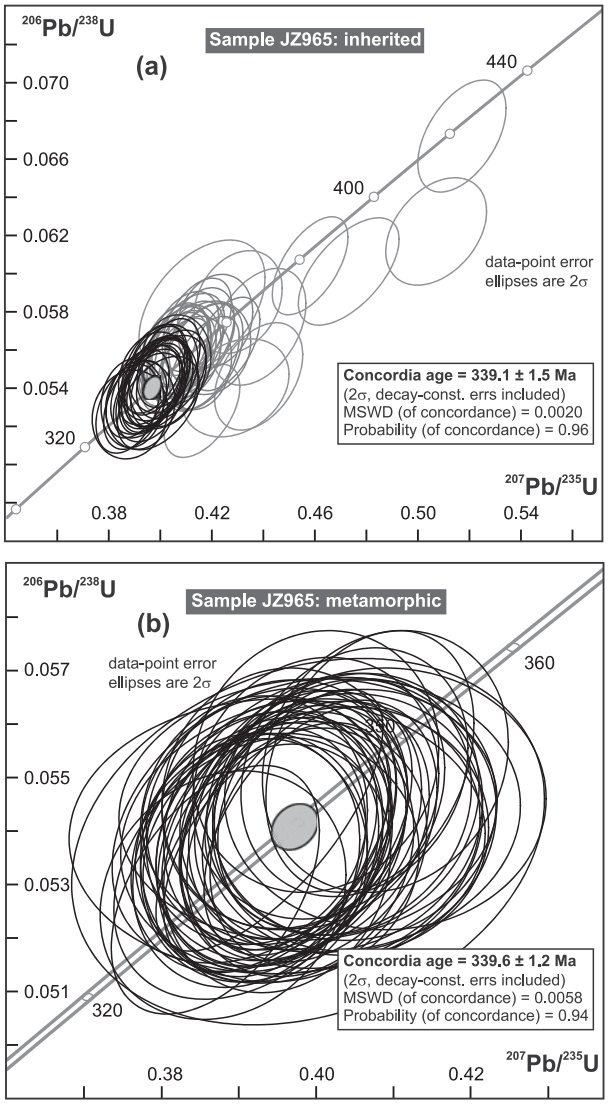

Figure 18. Concordia diagrams for sample JZ965 with (a) inherited and (b) metamorphic zircon weighted mean (concordia) Pb/U ages. The grey ellipses in (a) were not included in the calculation of the respective concordia age.

Babuška & Plomerová, 2013; Faryad & Kachlík, 2013; Zulauf *et al.* 2015); (2) the significance of the ubiquitous *c.* 340 Ma ages in granulites, that is, whether they represent maximum burial during crustal subduction or thickening or only a mid-crustal overprint on their retrograde path (e.g. Roberts & Finger, 1997; Kotková, 2007; Faryad, Nahodilová & Dolejš, 2010); (3) the heat source and trigger for the *c.* 340–335 Ma magmatism and coeval deformation (e.g. Henk *et al.* 2000), that is, whether elevated heat flow was caused by intracrustal radiogenic heating (Lexa *et al.* 2011; Schulmann *et al.* 2014), by input of hot mantle-derived melts after slab break-off or subcrustal mantle delamination (e.g. Stelltenpohl *et al.* 1993; Schaltegger, 1997; Willner *et al.* 2002; Massonne, 2006; Faryad *et al.* 2015), or by rifting related to incision of the Palaeo-Tethys Ocean into the orogen (Franke *et al.* 2011; Franke, 2014); and, last but not least, (4) evolution of surface palaeo-elevation, that is, whether this event was associated with the gravitational collapse of an orogenic plateau (Dörr & Zulauf, 2010, 2012) or the upper crust was only at low, near sea-level elevations (Franke, 2012, 2014).

Although it is beyond the scope of this paper to critically review details of all the models outlined above, our study of the Podolsko complex may add some new constraints on the Variscan *c.* 340 Ma event. Firstly, the extensive resetting of the U–Pb isotopic system in zircons from different units, including the retrogressed granulites within the migmatitic flat fabric (sample JZ965; Fig. 18), implies that the 340 Ma age post-dates the inferred high-pressure–low-temperature metamorphic peak and dates the mid-crustal, low-pressure–high-temperature overprint instead (Fig. 19a). Secondly, temperatures required to cause such extensive isotopic resetting (i.e. annealing of metamictized zircon lattice accompanied by more or less efficient lead loss) must have exceeded *c.* 600–650 °C according to experimental and analytical studies (Mezger & Krogstad, 1997; Geisler & Tomaschek, 2007; Schoene, 2014). It would be difficult to reach such high temperatures at relatively shallow depths exclusively by intracrustal radiogenic heating (e.g. Gerdes, Wörner & Finger, 2000; Lexa *et al.* 2011), an inference that favours a heat input from the underlying mantle during crustal thinning and collapse (this study) to cause the thermal anomaly (e.g. Henk *et al.* 2000; Dörr & Zulauf, 2010; Faryad *et al.* 2015). Last but not least, the normal shearing accommodating downdrop of the Teplá–Barrandian upper crust and extensional unroofing of the Podolsko complex (Fig. 19) juxtaposed crustal levels corresponding to pressures of *c.* 0.2–0.3 GPa (*c.* 8–10 km) and 0.5 GPa (*c.* 18 km), respectively (Žák *et al.* 2012; Faryad & Žák, 2016). The pressure difference therefore indicates a minimum throw along the Červená shear zone of *c.* 8–10 km, an estimate which is consistent with that proposed earlier by Zulauf *et al.* (2002) and Dörr & Zulauf (2010). The inferred minimum throw therefore provides a supporting argument for excess crustal thickness and significant palaeotopography in the interior of the Variscan orogenic belt during early Carboniferous time.

8. Conclusions

(1) The Podolsko complex was at least partly derived from Early Ordovician (*c.* 480 Ma) felsic igneous crust, the same age as inferred for melting the proto-source of the metapelitic migmatites of the Varied 'series'. These ages are interpreted as recording the Cambro-Ordovician rifting widespread across the Cadomian basement of the Bohemian Massif.

(2) Relics of the HP–UHP rocks suggest that at least some portions of the complex witnessed an early Variscan subduction to mantle depths and low-temperature eclogite-facies metamorphism. This was followed by pervasive anatexis at mid-crustal levels at *c.* 340–339 Ma. Most of our new U–Pb ages reflect the latter event.

https://doi.org/10.1017/S0016756816000030 Published online by Cambridge University Press

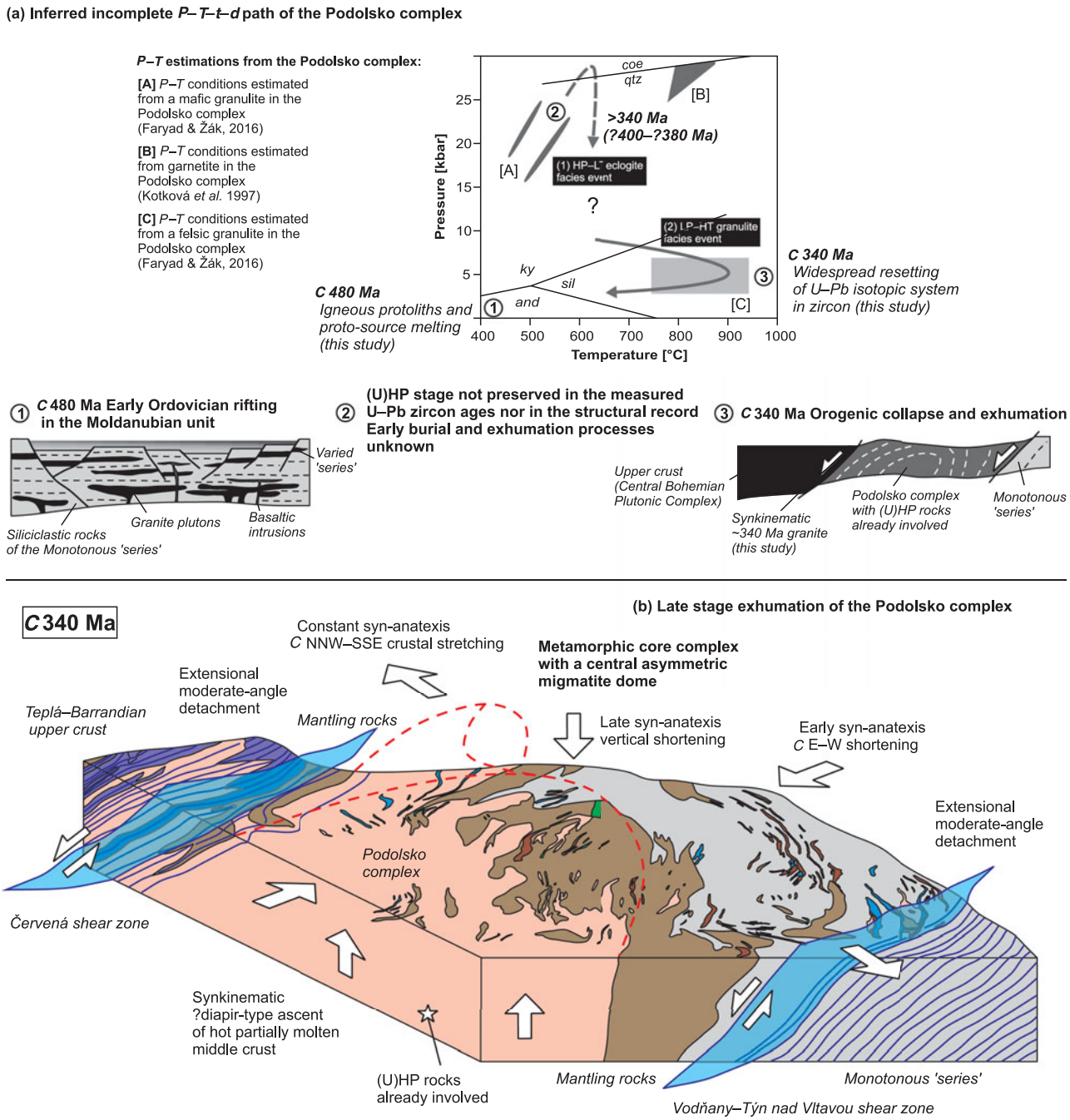

Figure 19. (Colour online) (a) Inferred, and certainly incomplete *P–T–t–d* path of the Podolsko complex and its metasedimentary mantling rocks showing its protracted tectonometamorphic history before and during the Variscan orogeny. The *P–T* estimations are from Faryad & Žák (2016). (b) Interpretive block diagram showing a late-stage exhumation of the Podolsko complex at *c.* 340 Ma as an asymmetric granite–migmatite dome flanked by crustal-scale normal detachments. See text for discussion.

(3) The Podolsko complex developed as an asymmetric dome cored by hot migmatites–granites during lateral *c.* E–W shortening and *c.* NNW–SSE stretching, perhaps by a combination of buoyancy and lateral tectonic forces. The dome then collapsed vertically and its further exhumation was taken over by crustal-scale extensional detachments. One of these detachments separates the upper crust from the deep-crustal interior of the orogen. These inferences are at variance with a previous interpretation of the complex as part of the extensive SE-directed 'Gföhl' nappe.

(4) The *c.* 340 Ma U–Pb ages detected in the Podolsko complex and its mantling rocks have also been reported from other segments of the Variscan orogenic belt. It could be deduced from our data that the 340 Ma age post-dates the high-pressure metamorphic peak, the temperatures required to cause the observed isotopic resetting of zircon must have been relatively high (probably reflecting heat input from the underlying mantle) and, finally, that the extensional unroofing of the complex requires a minimum throw of *c.* 8–10 km to juxtapose the contrasting crustal levels. We use this as an additional argument for excess crustal thickness

https://doi.org/10.1017/S0016756816000030 Published online by Cambridge University Press

and significant early Carboniferous palaeotopography in the interior of the Variscan orogen.

Acknowledgements. We thank an anonymous reviewer for the detailed and constructive comments and Editor Mark Allen for his careful editorial handling. We also thank Shah Wali Faryad for discussions and for sharing his *P–T* estimations of the Podolsko complex granulites. František Veselovský is thanked for the mineral separations. This study was supported by the Grant Agency of Charles University through Grant No. 906513 (to Miroslav Burjak) and by Charles University project PRVOUK P44.

Supplementary material

To view supplementary material for this article, please visit http://dx.doi.org/10.1017/S0016756816000030.

References

ACKERMAN, L., PAŠAVA, J. & ERBAN, V. 2013. Re–Os geochemistry and geochronology of the Ransko gabbro–peridotite massif, Bohemian Massif. *Mineralium Deposita* **48**, 799–804.

ALTHERR, R., HENES-KLAIBER, U., HEGNER, E., SATIR, M. & LANGER, C. 1999. Plutonism in the Variscan Odenwald (Germany): from subduction to collision. *International Journal of Earth Sciences* **88**, 422–43.

ASCH, K. 2003. The 1:5 million international geological map of Europe and adjacent areas: development and implementation of a GIS-enabled concept. Geologisches Jahrbuch, Sonderhefte, A3. E. Stuttgart: Schweizerbart Publishers.

BABUŠKA, V. & PLOMEROVÁ, J. 2013. Boundaries of mantle-lithosphere domains in the Bohemian Massif as extinct exhumation channels for high-pressure rocks. *Gondwana Research* **23**, 973–87.

BALLÉVRE, M., BOSSE, V., DUCASSOU, C. & PITRA, P. 2009. Palaeozoic history of the Armorican Massif: models for the tectonic evolution of the suture zones. *Comptes Rendus Geoscience* **341**, 174–201.

BEARD, B. L., MEDARIS, L. G., JOHNSON, C. M., BRUECKNER, H. K. & MÍSAŘ, Z. 1992. Petrogenesis of Variscan high-temperature Group A eclogites from the Moldanubian Zone of the Bohemian Massif, Czechoslovakia. *Contributions to Mineralogy and Petrology* **111**, 468–83.

BEAUMONT, C., JAMIESON, R. A., NGUYEN, M. H. & LEE, B. 2001. Himalayan tectonics explained by extrusion of a low-viscosity crustal channel coupled to focused surface denudation. *Nature* **414**, 738–42.

BORRADAILE, G. & HENRY, B. 1997. Tectonic applications of magnetic susceptibility and its anisotropy. *Earth-Science Reviews* **42**, 49–93.

BORRADAILE, G. J. & JACKSON, M. 2010. Structural geology, petrofabrics and magnetic fabrics (AMS, AARM, AIRM). *Journal of Structural Geology* **32**, 1519–51.

BRUECKNER, H. K., MEDARIS, L. G. & BAKUN-CZUBARÓW, N. 1991. Nd and Sr age isotope patterns from Variscan eclogites of the eastern Bohemian Massif. *Neues Jahrbuch für Mineralogie, Abhandlungen* **163**, 169–96.

BRUN, J. P. & VAN DEN DRIESSCHE, J. 1994. Extensional gneiss domes and detachment fault systems: structure and kinematics. *Bulletin de la Société Géologique de France* **165**, 519–30.

CARRERAS, J. & CAPELLA, I. 1994. Tectonic levels in the Palaeozoic basement of the Pyrenees: a review and a new interpretation. *Journal of Structural Geology* **16**, 1509–24.

CARSWELL, D. A. & O'BRIEN, P. J. 1993. Thermobarometry and geotectonic significance of high-pressure granulites: examples from the Moldanubian Zone of the Bohemian Massif in Lower Austria. *Journal of Petrology* **34**, 427–59.

CHARLES, N., FAURE, M. & CHEN, Y. 2009. The Montagne Noire migmatitic dome emplacement (French Massif Central): new insights from petrofabric and AMS studies. *Journal of Structural Geology* **31**, 1423–40.

COOKE, R. A. & O'BRIEN, P. J. 2001. Resolving the relationship between high P–T rocks and gneisses in collisional terranes: an example from the Gföhl gneiss–granulite association in the Moldanubian Zone, Austria. *Lithos* **58**, 33–54.

COSTA, S. & REY, P. F. 1995. Lower crustal rejuvenation and growth during post-thickening collapse: insights from a crustal cross section through a Variscan metamorphic core complex. *Geology* **23**, 905–8.

CROWLEY, Q. G., FLOYD, P. A., WINCHESTER, J. A., FRANKE, W. & HOLLAND, J. G. 2000. Early Palaeozoic reft-related magmatism in Variscan Europe: fragmentation of the Armorican Terrane Assemblage. *Terra Nova* **12**, 171–80.

CULSHAW, N. G., BEAUMONT, C. & JAMIESON, R. A. 2006. The orogenic superstructure–infrastructure concept: revisited, quantified, and revived. *Geology* **34**, 733–6.

DE SITTER, L. U. & ZWART, H. J. 1960. Tectonic development in supra and infra-structures of a mountain chain. *Proceedings of the 21st International Geological Congress*, Copenhagen, pp. 248–56.

DEWEY, J. F. 1988. Extensional collapse of orogens. *Tectonics* **7**, 1123–39.

DOBRZHINETSKAYA, L. F. & FARYAD, S. W. 2011. Frontiers of ultrahigh-pressure metamorphism: view from field and laboratory. In *Ultrahigh-Pressure Metamorphism: 25 Years after the Discovery of Coesite and Diamond* (eds L. F. Dobrzhinetskaya, S. W. Faryad, S. Wallis & S. Cuthbert), pp. 1–39. Amsterdam: Elsevier.

DÖRR, W. & ZULAUF, G. 2010. Elevator tectonics and orogenic collapse of a Tibetan-style plateau in the European Variscides: the role of the Bohemian shear zone. *International Journal of Earth Sciences* **99**, 299–325.

DÖRR, W. & ZULAUF, G. 2012. Reply to W. Franke on W. Dörr and G. Zulauf elevator tectonics and orogenic collapse of a Tibetan-style plateau in the European Variscides: the role of the Bohemian shear zone. *International Journal of Earth Sciences* **101**, 2035–41.

DOSTAL, J., PATOČKA, F. & PIN, C. 2001. Middle/Late Cambrian intracontinental rifting in the central West Sudetes, NE Bohemian Massif (Czech Republic): geochemistry and petrogenesis of bimodal volcanic rocks. *Geological Journal* **36**, 1–17.

FARYAD, S. W. & KACHLÍK, V. 2013. New evidence of blueschist facies rocks and their geotectonic implication for Variscan suture(s) in the Bohemian Massif. *Journal of Metamorphic Geology* **31**, 63–82.

FARYAD, S. W., KACHLÍK, V., SLÁMA, J. & HOINKES, G. 2015. Implication of corona formation in a metatroctolite to the granulite facies overprint of HP–UHP rocks in the Moldanubian Zone (Bohemian Massif). *Journal of Metamorphic Geology* **33**, 295–310.

FARYAD, S. W., NAHODILOVÁ, R. & DOLEJŠ, D. 2010. Incipient eclogite facies metamorphism in the Moldanubian granulites revealed by mineral inclusions in garnet. *Lithos* **114**, 54–69.

FARYAD, S. W. & ŽÁK, J. 2016. High-pressure granulites of the Podolsko complex, Bohemian Massif: an example of crustal rocks that were subducted to mantle depths and survived a pervasive mid-crustal high-temperature overprint. *Lithos*, doi: 10.1016/j.lithos.2016.01.005.

FEDIUKOVÁ, E. & FEDIUK, F. 1971. Moldanubian granulites of the Písek–Týn area. *Acta Universitatis Carolinae, Geologica* **1**, 25–47.

FERRÉ, E. C., TEYSSIER, C., JACKSON, M., HILL, J. W. & RAINEY, E.S.G. 2002. Magnetic susceptibility anisotropy: a new petrofabric tool in migmatites. *Journal of Geophysical Research* **108**, 2086, doi: 10.1029/2002JB001790.

FINGER, F., GERDES, A., JANOUŠEK, V., RENÉ, M. & RIEGLER, G. 2007. Resolving the Variscan evolution of the Moldanubian sector of the Bohemian Massif: the significance of the Bavarian and the Moravo–Moldanubian tectonometamorphic phases. *Journal of Geosciences* **52**, 9–28.

FINGER, F. & KRENN, E. 2007. Three metamorphic monazite generations in a high-pressure rock from the Bohemian Massif and the potentially important role of apatite in stimulating polyphase monazite growth along a PT loop. *Lithos* **95**, 103–15.

FIŠERA, M., VRÁNA, S. & KOTRBA, Z. 1982. Orthopyroxene–garnet granulites in the Podolsko complex. *Bulletin of the Geological Survey, Prague* **57**, 321–8.

FRANĚK, J., SCHULMANN, K. & LEXA, O. 2006. Kinematic and rheological model of exhumation of high pressure granulites in the Variscan orogenic root: example of the Blanský les granulite, Bohemian Massif, Czech Republic. *Mineralogy and Petrology* **86**, 253–76.

FRANĚK, J., SCHULMANN, K., LEXA, O., TOMEK, C. & EDEL, J. B. 2011. Model of syn-convergent extrusion of orogenic lower crust in the core of the Variscan belt: implications for exhumation of high-pressure rocks in large hot orogens. *Journal of Metamorphic Geology* **29**, 53–78.

FRANKE, W. 1999. Tectonic and plate tectonic units at the north Gondwana margin: evidence from the Central European Variscides. *Abhandlungen der Geologischen Bundesanstalt* **54**, 7–13.

FRANKE, W. 2000. The mid-European segment of the Variscides: tectonostratigraphic units, terrane boundaries and plate tectonic evolution. In *Orogenic Processes: Quantification and Modelling in the Variscan Belt* (eds W. Franke, V. Haak, O. Oncken & D. Tanner), pp. 35–61. Geological Society, London, Special Publication no. 179.

FRANKE, W. 2006. The Variscan orogen in Central Europe: construction and collapse. In *European Litosphere Dynamics* (eds by D. G. Gee & R. A. Stephenson), pp. 333–43. Geological Society, London, Memoir no. 32.

FRANKE, W. 2012. Comment on Dörr and Zulauf: elevator tectonics and orogenic collapse of a Tibetan-style plateau in the European Variscides: the role of the Bohemian shear zone. Int J Earth Sci (Geol Rundsch) (2010) 99: 299–325. *International Journal of Earth Sciences* **101**, 2027–34.

FRANKE, W. 2014. Topography of the Variscan orogen in Europe: failed – not collapsed. *International Journal of Earth Sciences* **103**, 1471–99.

FRANKE, W., DOUBLIER, M. P., KLAMA, K., POTEL, S. & WEMMER, K. 2011. Hot metamorphic core complex in a cold foreland. *International Journal of Earth Sciences* **100**, 753–85.

GEISLER, T. & TOMASCHEK, F. 2007. Re-equilibration of zircon in aqueous fluids and melts. *Elements* **3**, 43–50.

GERDES, A., WÖRNER, G. & FINGER, F. 2000. Hybrids, magma mixing and enriched mantle melts in post-collisional Variscan granitoids: the Rastenberg Pluton, Austria. In *Orogenic Processes: Quantification and Modelling in the Variscan Belt* (eds W. Franke, V. Haak, O. Oncken & D. Tanner), pp. 415–31. Geological Society, London, Special Publication no. 179.

GIACOMINI, F., DALLAI, L., CARMINATI, E., TIEPOLO, M. & GHEZZO, C. 2008. Exhumation of a Variscan orogenic complex: insights into the composite granulitic–amphibolitic metamorphic basement of south-east Corsica (France). *Journal of Metamorphic Geology* **26**, 403–36.

HENK, A., VON BLANCKENBURG, F., FINGER, F., SCHALTEGGER, U. & ZULAUF, G. 2000. Syn-convergent high-temperature metamorphism and magmatism in the Variscides: a discussion of potential heat sources. In: *Orogenic Processes: Quantification and Modelling in the Variscan Belt* (eds W. Franke, V. Haak, O. Oncken & D. Tanner), pp. 387–99. Geological Society, London, Special Publication no. 179.

HENRY, B. 1997. The magnetic zone axis: a new element of magnetic fabric for the interpretation of the magnetic lineation. *Tectonophysics* **271**, 325–31.

HOLUB, F. V. 1997. Ultrapotassic plutonic rocks of the durbachite series in the Bohemian Massif: petrology, geochemistry, and petrogenetic interpretation. *Journal of Geological Sciences, Economic Geology, Mineralogy* **31**, 5–26.

HOLUB, F. V., COCHERIE, A. & ROSSI, P. 1997. Radiometric dating of granitic rocks from the Central Bohemian Plutonic Complex: constraints on the chronology of thermal and tectonic events along the Barrandian–Moldanubian boundary. *Comptes Rendus de L'Academie des Sciences - Series IIA - Earth and Planetary Science* **325**, 19–26.

HOLUB, F. V., VERNER, K. & SCHMITZ, M. D. 2011. Temporal relations of melagranite porphyry dykes and durbachitic plutons in South Bohemia. *Geoscience Research Reports* **2011**, 23–5.

HROUDA, F. 1982. Magnetic anisotropy of rocks and its application in geology and geophysics. *Geophysical Surveys* **5**, 37–82.

HROUDA, F. 1994. A technique for the measurement of thermal changes of magnetic susceptibility of weakly magnetic rocks by the CS-2 apparatus and KLY-2 Kappabridge. *Geophysical Journal International* **118**, 604–12.

HROUDA, F. & KAHAN, Š. 1991. The magnetic fabric relationship between sedimentary and basement nappes in the High Tatra Mountains, N. Slovakia. *Journal of Structural Geology* **13**, 431–42.

JACKSON, S. E., PEARSON, N. J., GRIFFIN, W. L. & BELOUSOVA, E. A. 2004. The application of laser ablation-inductively coupled plasma-mass spectrometry to in situ U–Pb zircon geochronology. *Chemical Geology* **211**, 47–69.

JAMIESON, R. A. & BEAUMONT, C. 2013. On the origin of orogens. *Geological Society of America Bulletin* **125**, 1671–702.

JANOUŠEK, V. & GERDES, A. 2003. Timing the magmatic activity within the Central Bohemian Pluton, Czech Republic: conventional U–Pb ages for the Sázava and Tábor intrusions and their geotectonic significance. *Journal of the Czech Geological Society* **48**, 70–1.

JANOUŠEK, V. & HOLUB, F. 2007. The causal link between HP–HT metamorphism and ultrapotassic magmatism in collisional orogens: case study from the Moldanubian

Zone of the Bohemian Massif. *Proceedings of the Geologists' Association* **118**, 75–86.

JELÍNEK, V. 1978. Statistical processing of anisotropy of magnetic susceptibility measured on groups of specimens. *Studia Geophysica et Geodetica* **22**, 50–62.

JELÍNEK, V. 1981. Characterization of the magnetic fabric of rocks. *Tectonophysics* **79**, T63–7.

KACHLÍK, V. & PATOČKA, F. 1998. Cambrian/Ordovician intracontinental rifting and Devonian closure of the rifting generated basins in the Bohemian Massif realms. *Acta Universitatis Carolinae, Geologica* **42**, 433–41.

KLOMÍNSKÝ, J., JARCHOVSKÝ, T. & RAJPOOT, G. S. 2010. *Atlas of plutonic rocks and orthogneisses in the Bohemian Massif. 2. Moldanubicum.* Prague: Czech Geological Survey, 199 pp.

KONOPÁSEK, J., PILÁTOVÁ, E., KOŠLER, J. & SLÁMA, J. 2014. Zircon (re)crystallization during short-lived, high-P granulite facies metamorphism (Eger Complex, NW Bohemian Massif). *Journal of Metamorphic Geology* **32**, 885–902.

KOŠLER, J., ROGERS, G., RODDICK, J. C. & BOWES, D. R. 1995. Temporal association of ductile deformation and granitic plutonism: Rb–Sr and ^{40}Ar–^{39}Ar evidence from roof pendants above the Central Bohemian Pluton, Czech Republic. *Journal of Geology* **103**, 711–7.

KOTKOVÁ, J. 2007. High-pressure granulites of the Bohemian Massif: recent advances and open questions. *Journal of Geosciences* **52**, 45–71.

KOTKOVÁ, J., DÖRR, W. & FINGER, F. 1998. New geochemical and geochronological data on the very-high-pressure garnetite from the Podolsko Complex, Moldanubian Zone, Bohemian Massif. *Acta Universitatis Carolinae, Geologica* **42**, 281–2.

KOTKOVÁ, J., HARLEY, S. L. & FIŠERA, M. 1997. A vestige of very high-pressure (ca. 28 kbar) metamorphism in the Variscan Bohemian Massif, Czech Republic. *European Journal of Mineralogy* **9**, 1017–33.

KOTKOVÁ, J., KRÖNER, A., TODT, W. & FIALA, J. 1995. Zircon dating of North Bohemian granulites, Czech Republic: further evidence for the Lower Carboniferous high-pressure event in the Bohemian Massif. *Geologische Rundschau* **85**, 154–61.

KOTKOVÁ, J., SCHALTEGGER, U. & LEICHMANN, J. 2010. Two types of ultrapotassic plutonic rocks in the Bohemian Massif – coeval intrusions at different crustal levels. *Lithos* **115**, 163–76.

KRENN, E. & FINGER, F. 2004. Metamorphic formation of Sr-apatite and Sr-bearing monazite in a high-pressure rock from the Bohemian Massif. *American Mineralogist* **89**, 1323–9.

KRÖNER, A., JAECKEL, P., REISCHMANN, T. & KRONER, U. 1998. Further evidence for an early Carboniferous (~340 Ma) age of high-grade metamorphism in the Saxonian granulite complex. *Geologische Rundschau* **86**, 751–66.

KRÖNER, A., O'BRIEN, P. J., NEMCHIN, A. A. & PIDGEON, R. T. 2000. Zircon ages for high pressure granulites from South Bohemia, Czech Republic, and their connection to Carboniferous high temperature processes. *Contributions to Mineralogy and Petrology* **138**, 127–42.

KRONER, U. & ROMER, R. L. 2013. Two plates – many subduction zones: the Variscan orogeny reconsidered. *Gondwana Research* **24**, 298–329.

KRUCKENBERG, S. C., FERRÉ, E. C., TEYSSIER, C., VANDERHAEGHE, O., WHITNEY, D. L., SEATON, N. C. A. & SKORD, J. A. 2010. Viscoplastic flow in migmatites deduced from fabric anisotropy: an example from the Naxos dome, Greece. *Journal of Geophysical Research* **115**, B09401.

KRUCKENBERG, S. C., VANDERHAEGHE, O., FERRÉ, E. C., TEYSSIER, C. & WHITNEY, D. L. 2011. Flow of partially molten crust and the internal dynamics of a migmatite dome, Naxos, Greece. *Tectonics* **30**, TC3001.

KUSIAK, M. A., DUNKLEY, D. J., SUZUKI, K., KACHLÍK, V., KEDZIOR, A., LEKKI, J. & OPLUŠTIL, S. 2010. Chemical (non-isotopic) and isotopic dating of Phanerozoic zircon – a case study of durbachite from the Třebíč Pluton, Bohemian Massif. *Gondwana Research* **17**, 153–61.

LARDEAUX, J. M., SCHULMANN, K., FAURE, M., JANOUŠEK, V., LEXA, O., SKRZYPEK, E., EDEL, J. B. & ŠTÍPSKÁ, P. 2014. The Moldanubian Zone in the French Massif Central, Vosges/Schwarzwald and Bohemian Massif revisited: differences and similarities. In *The Variscan Orogeny: Extent, Timescale and the Formation of the European Crust* (eds K. Schulmann, J. R. Martínez Catalán, J. M. Lardeaux, V. Janoušek & G. Oggiano), pp. 7–44. Geological Society, London, Special Publication no. 405.

LEXA, O., SCHULMANN, K., JANOUŠEK, V., ŠTÍPSKÁ, P., GUY, A. & RACEK, M. 2011. Heat sources and trigger mechanisms of exhumation of HP granulites in Variscan orogenic root. *Journal of Metamorphic Geology* **29**, 79–102.

LINNER, M. 1996. Metamorphism and partial melting of paragneisses of the Monotonous Group, SE Moldanubicum (Austria). *Mineralogy and Petrology* **58**, 215–34.

LIOU, J. G., TSUJIMORI, T., YANG, J., ZHANG, R. Y. & ERNST, W. G. 2014. Recycling of crustal materials through study of ultrahigh–pressure minerals in collisional orogens, ophiolites, and mantle xenoliths: a review. *Journal of Asian Earth Sciences* **96**, 386–420.

LOBKOWICZ, M., ŠTĚDRÁ, V. & SCHULMANN, K. 1996. Late-Variscan extensional collapse of the thickened Moldanubian crust in the southern Bohemia. *Journal of the Czech Geological Society* **41**, 123–38.

LUDWIG, K. R. 2008. Isoplot 3.70. A geochronological toolkit for Microsoft Excel. Berkeley Geochronology Center, Special Publication no. 4.

MARTÍNEZ CATALÁN, J. R. 2011. Are the oroclines of the Variscan belt related to late Variscan strike-slip tectonics? *Terra Nova* **23**, 241–7.

MARTÍNEZ CATALÁN, J. R. 2012. The Central Iberian arc, an orocline centered in the Iberian Massif and some implications for the Variscan belt. *International Journal of Earth Sciences* **101**, 1299–314.

MASSONNE, H. J. 2006. Early metamorphic evolution and exhumation of felsic high-pressure granulites from the north-western Bohemian Massif. *Mineralogy and Petrology* **86**, 177–202.

MATTE, P. 2001. The Variscan collage and orogeny (480–290 Ma) and the tectonic definition of the Armorica microplate: a review. *Terra Nova* **13**, 122–8.

MATTE, P., MALUSKI, H., RAJLICH, P. & FRANKE, W. 1990. Terrane boundaries in the Bohemian Massif: result of large-scale Variscan shearing. *Tectonophysics* **177**, 151–70.

MEDARIS, L. G., BEARD, B. L. & JELÍNEK, E. 2006. Mantle-derived, UHP garnet pyroxenite and eclogite in the Moldanubian Gföhl nappe, Bohemian Massif: a geochemical review, new P–T determinations, and tectonic interpretation. *International Geology Review* **48**, 765–77.

MEDARIS, G., BEARD, B. L., JOHNSON, C. M., VALLEY, J. W., SPICUZZA, M. J., JELÍNEK, E. & MÍSAŘ, Z. 1995.

Garnet pyroxenite and eclogite in the Bohemian Massif: geochemical evidence for Variscan recycling of subducted lithosphere. *Geologische Rundschau* **84**, 489–505.

MEDARIS, G., WANG, H., JELÍNEK, E., MIHALJEVIČ, M. & JAKEŠ, P. 2005. Characteristics and origins of diverse Variscan peridotites in the Gföhl Nappe, Bohemian Massif, Czech Republic. *Lithos* **82**, 1–23.

MEZGER, K. & KROGSTAD, E. J. 1997. Interpretation of discordant U–Pb zircon ages: an evaluation. *Journal of Metamorphic Geology* **15**, 127–40.

MURPHY, D. C. 1987. Suprastructure/infrastructure transition, east central Cariboo Mountains, British Columbia: geometry, kinematics and tectonic implications. *Journal of Structural Geology* **9**, 13–29.

NANCE, R. D., GUTIERRÉZ-ALONSO, G., KEPPIE, J. D., LINNEMANN, U., MURPHY, J. B., QUESADA, C., STRACHAN, R. A. & WOODCOCK, N. H. 2010. Evolution of the Rheic Ocean. *Gondwana Research* **17**, 194–222.

O'BRIEN, P. J. & CARSWELL, D. A. 1993. Tectonometamorphic evolution of the Bohemian Massif: evidence from high pressure metamorphic rocks. *Geologische Rundschau* **82**, 531–55.

OWEN, J. V. & DOSTAL, J. 1996. Prograde metamorphism and decompression of the Gföhl gneiss, Czech Republic. *Lithos* **38**, 259–70.

PATON, C., WOODHEAD, J. D., HELLSTROM, J. C., HERGT, J. M., GREIG, A. & MAAS, R. 2010. Improved laser ablation U–Pb zircon geochronology through robust downhole fractionation correction. *Geochemistry Geophysics Geosystems* **11**, Q0AA06.

PETRAKAKIS, K. 1997. Evolution of Moldanubian rocks in Austria: review and synthesis. *Journal of Metamorphic Geology* **15**, 203–22.

PETRUS, J. A. & KAMBER, B. S. 2012. VizualAge: a novel approach to laser ablation ICP-MS U–Pb geochronology data reduction. *Geostandards and Geoanalytical Research* **36**, 247–70.

PHARAOH, T. C. 1999. Palaeozoic terranes and their lithospheric boundaries within the Trans-European Suture Zone (TESZ): a review. *Tectonophysics* **314**, 17–41.

PIN, C., KRYZA, R., OBERC-DZIEDZIC, T., MAZUR, S., TURNIAK, K. & WALDHAUSROVÁ, J. 2007. The diversity and geodynamic significance of Late Cambrian (ca. 500 Ma) felsic anorogenic magmatism in the northern part of the Bohemian Massif: a review based on Sm–Nd isotope and geochemical data. In *The Evolution of the Rheic Ocean: From Avalonian–Cadomian Active Margin to Alleghenian–Variscan Collision* (eds U. Linnemann, R. D. Nance, P. Kraft & G. Zulauf), pp. 209–29. Geological Society of America, Special Paper no. 423.

PITRA, P., BURG, J. P. & GUIRAUD, M. 1999. Late Variscan strike-slip tectonics between the Teplá–Barrandian and Moldanubian terranes (Czech Bohemian Massif): petrostructural evidence. *Journal of the Geological Society, London* **156**, 1003–20.

PITRA, P., BURG, J. P., SCHULMANN, K. & LEDRU, K. 1994. Late orogenic extension in the Bohemian Massif: petrostructural evidence in the Hlinsko region. *Geodynamica Acta* **7**, 15–30.

PLATT, J. P., BEHR, W. M. & COOPER, F. J. 2014. Metamorphic core complexes: windows into the mechanics and rheology of the crust. *Journal of the Geological Society, London* **172**, 9–27.

PLATT, J. P., WHITEHOUSE, M. J., KELLEY, S. P., CARTER, A. & HOLLICK, L. 2003. Simultaneous extensional exhumation across the Alboran Basin: implications for the causes of late orogenic extension. *Geology* **31**, 251–4.

RENÉ, M. 2006. Provenance studies of Moldanubian paragneisses based on geochemical data (Bohemian Massif, Czech Republic). *Neues Jahrbuch für Geologie and Paläntologie, Abhandlungen* **242**, 83–101.

REY, P. F., TEYSSIER, C., KRUCKENBERG, S. C. & WHITNEY, D. L. 2011. Viscous collision in channel explains double domes in metamorphic core complexes. *Geology* **39**, 387–90.

REY, P. F., TEYSSIER, C. & WHITNEY, D. L. 2009*a*. Extension rates, crustal melting, and core complex dynamics. *Geology* **37**, 391–4.

REY, P. F., TEYSSIER, C. & WHITNEY, D. L. 2009*b*. The role of partial melting and extensional strain rates in the development of metamorphic core complexes. *Tectonophysics* **477**, 134–44.

REY, P. F., TEYSSIER, C. & WHITNEY, D. L. 2010. Limit of channel flow in orogenic plateaux. *Lithosphere* **2**, 328–32.

REY, P. F., VANDERHAEGHE, O. & TEYSSIER, C. 2001. Gravitational collapse of the continental crust: definition, regimes and modes. *Tectonophysics* **342**, 435–49.

RIVERS, T. 2012. Upper-crustal orogenic lid and mid-crustal core complexes: signature of a collapsed orogenic plateau in the hinterland of the Grenville Province. *Canadian Journal of Earth Sciences* **49**, 1–42.

ROBERTS, M. P. & FINGER, F. 1997. Do U–Pb zircon ages from granulites reflect peak metamorphic conditions? *Geology* **25**, 319–22.

ROCHETTE, P., JACKSON, M. & AUBOURG, C. 1992. Rock magnetism and the interpretation of anisotropy of magnetic susceptibility. *Reviews of Geophysics* **30**, 209–26.

ROGER, F., TEYSSIER, C., RESPAUT, J. P., REY, P. F., JOLIVET, M., WHITNEY, D. L., PAQUETTE, J. L. & BRUNEL, M. 2015. Timing of formation and exhumation of the Montagne Noire double dome, French Massif Central. *Tectonophysics* **640–641**, 53–69.

RÖHLICHOVÁ, M. 1962. On enclaves and blocks in the Podolsko complex in the eastern vicinity of Písek. *Journal for Mineralogy and Geology* **3**, 301–6.

RÖHLICHOVÁ, M. 1963. Migmatites of the Podolsko complex in the Písek area. *Acta Universitatis Carolinae, Geologica* **3**, 197–210.

ROMER, R. L. & RÖTZLER, J. 2001. P–T–t evolution of ultrahigh-temperature granulites from the Saxon Granulite Massif, Germany. Part II: geochronology. *Journal of Petrology* **42**, 2015–32.

RUBATTO, D., FERRANDO, S., COMPAGNONI, R. & LOMBARDO, B. 2010. Carboniferous high-pressure metamorphism of Ordovician protoliths in the Argentera Massif (Italy), Southern European Variscan belt. *Lithos* **116**, 65–76.

SCHALTEGGER, U. 1997. Magma pulses in the Central Variscan Belt: episodic melt generation and emplacement during litospheric thinning. *Terra Nova* **9**, 242–5.

SCHALTEGGER, U., SCHNEIDER, J. L., MAURIN, J. C. & CORFU, F. 1996. Precise U–Pb chronometry of 345–340 Ma old magmatism related to syn-convergence extension in the Southern Vosges (Central Variscan Belt). *Earth and Planetary Science Letters* **144**, 403–19.

SCHEUVENS, D. & ZULAUF, G. 2000. Exhumation, strain localization, and emplacement of granitoids along the western part of the Central Bohemian shear zone (Bohemian Massif). *International Journal of Earth Sciences* **89**, 617–30.

SCHOENE, B. 2014. U–Th–Pb geochronology. In *Treatise on Geochemistry (2nd Edition)* (eds H. Holland & K. Turejian), pp. 341–78. Amsterdam: Elsevier.

SCHULMANN, K., EDEL, J. B., HASALOVÁ, P., COSGROVE, J. W., JEŽEK, J. & LEXA, O. 2009*a*. Influence of melt induced mechanical anisotropy on the magnetic fabrics and rheology of deforming migmatites, Central Vosges, France. *Journal of Structural Geology* **31**, 1223–37.

SCHULMANN, K., KONOPÁSEK, J., JANOUŠEK, V., LEXA, O., LARDEAUX, J. M., EDEL, J. B., ŠTÍPSKÁ, P. & ULRICH, S. 2009*b*. An Andean type Palaeozoic convergence in the Bohemian Massif. *Comptes Rendus Geoscience* **341**, 266–86.

SCHULMANN, K., LEXA, O., JANOUŠEK, V., LARDEAUX, J. M. & EDEL, J. B. 2014. Anatomy of a diffuse cryptic suture zone: an example from the Bohemian Massif, European Variscides. *Geology* **42**, 275–8.

SKRZYPEK, E., SCHULMANN, K., TABAUD, A. S. & EDEL, J. B. 2014. Palaeozoic evolution of the Variscan Vosges Mountains. In *The Variscan Orogeny: Extent, Timescale and the Formation of the European Crust* (eds K. Schulmann, J. R. Martínez Catalán, J. M. Lardeaux, V. Janoušek & G. Oggiano), pp. 45–75. Geological Society, London, Special Publication no. 405.

SKRZYPEK, E., ŠTÍPSKÁ, P. & COCHERIE, A. 2012. The origin of zircon and the significance of U–Pb ages in high-grade metamorphic rocks: a case study from the Variscan orogenic root (Vosges Mountains, NE France). *Contributions to Mineralogy and Petrology* **164**, 935–57.

SLÁMA, J., KOŠLER, J., CONDON, D. J., CROWLEY, J. L., GERDES, A., HANCHAR, J. M., HORSTWOOD, M. S. A., MORRIS, G. A., NASDALA, L., NORBERG, N., SCHALTEGGER, U., SCHOENE, B., TUBRETT, M. N. & WHITEHOUSE, M. J. 2008. Plešovice zircon – a new natural reference material for U–Pb and Hf isotopic microanalysis. *Chemical Geology* **249**, 1–35.

STELTENPOHL, M. G., CYMERMAN, Z., KROGH, E. J. & KUNK, M. J. 1993. Exhumation of eclogitized continental basement during Variscan lithospheric delamination and gravitational collapse, Sudety Mountains, Poland. *Geology* **21**, 1111–4.

TABAUD, A. S., JANOUŠEK, V., SKRZYPEK, E., SCHULMANN, K., ROSSI, P., WHITECHURCH, H., GUERROT, C. & PAQUETTE, J. L. 2014. Chronology, petrogenesis and heat sources for successive Carboniferous magmatic events in the Southern–Central Variscan Vosges Mts (NE France). *Journal of the Geological Society, London* **172**, 87–102.

TAIT, J., SCHÄTZ, M., BACHTADSE, V. & SOFFEL, H. 2000. Palaeomagnetism and Palaeozoic palaeogeography of Gondwana and European terranes. In *Orogenic Processes: Quantification and Modelling in the Variscan Belt* (eds W. Franke, V. Haak, O. Oncken & D. Tanner), pp. 21–34. Geological Society, London, Special Publication no. 179.

TARLING, D. H. & HROUDA, F. 1993. *The Magnetic Anisotropy of Rocks*. London: Chapman and Hall, 217 pp.

TIREL, C., BRUN, J. P. & BUROV, E. 2004. Thermomechanical modeling of extensional gneiss domes. In *Gneiss Domes in Orogeny* (eds D. L. Whitney, C. Teyssier & C. S. Siddoway), pp. 67–78. Geological Society of America, Special Paper no. 380.

TOLLMANN, A. 1982. Large-scale nappe structure of the Moldanubian and new ideas on the European Variscides. *Geotektonische Forschungen* **64**, 1–91.

TOMEK, F., ŽÁK, J. & CHADIMA, M. 2015. Granitic magma emplacement and deformation during early-orogenic syn-convergent transtension: the Staré Sedlo complex, Bohemian Massif. *Journal of Geodynamics* **87**, 50–66.

URBAN, K. 1930. Geology of an area near confluence of the Vltava and Otava Rivers. *Bulletin of the State Geological Institute* **9**, 109–64.

VIEGAS, L. G. F., ARCHANJO, C. J. & VAUCHEZ, A. 2013. Fabrics of migmatites and the relationships between partial melting and deformation in high-grade transpressional shear zones: the Espinho Branco anatexite (Borborema Province, NE Brazil). *Journal of Structural Geology* **48**, 45–56.

VON RAUMER, J. F., BUSSY, F., SCHALTEGGER, U., SCHULZ, B. & STAMPFLI, G. M. 2013. Pre-Mesozoic Alpine basements – their place in the European Paleozoic framework. *Geological Society of America Bulletin* **125**, 89–108.

VON RAUMER, J. F., FINGER, F., VESELÁ, P. & STAMPFLI, G. M. 2014. Durbachites–vaugnerites – a geodynamic marker in the central European Variscan orogen. *Terra Nova* **26**, 85–95.

VRÁNA, S. 1979. Polyphase shear folding and thrusting in the Moldanubicum of southern Bohemia. *Bulletin of the Central Geological Survey* **54**, 75–86.

VRÁNA, S. 1988. The Moldanubian zone in southern Bohemia: polyphase evolution of imbricated crustal and upper mantle segments. *Proceedings of the 1st International Conference on the Bohemian Massif*, Prague, pp. 331–6.

WHITNEY, D. L., ROGER, F., TEYSSIER, C., REY, P. F. & RESPAUT, J. P. 2015. Syn-collapse eclogite metamorphism and exhumation of deep crust in a migmatite dome: the P–T–t record of the youngest Variscan eclogite (Montagne Noire, French Massif Central). *Earth and Planetary Science Letters* **430**, 224–34.

WHITNEY, D. L., TEYSSIER, C., REY, P. F. & BUCK, R. W. 2013. Continental and oceanic core complexes. *Geological Society of America Bulletin* **125**, 273–98.

WIEDENBECK, M., ALLE, P., CORFU, F., GRIFFIN, W. L., MEIER, M., OBERLI, F., VON QUADT, A., RODDICK, J. C. & SPEIGEL, W. 1995. Three natural zircon standards for U–Th–Pb, Lu–Hf, trace-element and REE analyses. *Geostandards Newsletter* **19**, 1–23.

WILLNER, A. P., SEBAZUNGU, E., GERYA, T. V., MARESCH, W. V. & KROHE, A. 2002. Numerical modelling of PT-paths related to rapid exhumation of high-pressure rocks from the crustal root in the Variscan Erzgebirge Dome (Saxony/Germany). *Journal of Geodynamics* **33**, 281–314.

WINCHESTER, J. A. 2002. Palaeozoic amalgamation of Central Europe: new results from recent geological and geophysical investigations. *Tectonophysics* **360**, 5–21.

WINCHESTER, J. A., PHARAOH, T. C., VERNIERS, J., IOANE, D. & SEGHEDI, A. 2006. Palaeozoic accretion of Gondwana-derived terranes to the East European Craton: recognition of detached terrane fragments dispersed after collision with promontories. In *European Litosphere Dynamics* (eds by D. G. Gee & R. A. Stephenson), pp. 323–32. Geological Society, London, Memoir no. 32.

ŽÁK, J., HOLUB, F. V. & VERNER, K. 2005. Tectonic evolution of a continental magmatic arc from transpression in the upper crust to exhumation of mid-crustal orogenic root recorded by episodically emplaced plutons: the Central Bohemian Plutonic Complex (Bohemian Massif). *International Journal of Earth Sciences* **94**, 385–400.

ŽÁK, J., KRAFT, P. & HAJNÁ, J. 2013. Timing, styles, and kinematics of Cambro–Ordovician extension in the Teplá–Barrandian Unit, Bohemian Massif, and its bearing on the opening of the Rheic Ocean. *International Journal of Earth Sciences* **102**, 415–33.

ŽÁK, J., VERNER, K., HOLUB, F. V., KABELE, P., CHLUPÁČOVÁ, M. & HALODOVÁ, P. 2012. Magmatic to solid state fabrics in syntectonic granitoids recording early Carboniferous orogenic collapse in the Bohemian Massif. *Journal of Structural Geology* **36**, 27–42.

ŽÁK, J., VERNER, K., JANOUŠEK, V., HOLUB, F. V., KACHLÍK, V., FINGER, F., HAJNÁ, J., TOMEK, F., VONDROVIC, L. & TRUBAČ, J. 2014. A plate-kinematic model for the assembly of the Bohemian Massif constrained by structural relationships around granitoid plutons. In *The Variscan Orogeny: Extent, Timescale and the Formation of the European Crust* (eds K. Schulmann, J. R. Martínez Catalán, J. M. Lardeaux, V. Janoušek & G. Oggiano), pp. 169–96. Geological Society, London, Special Publication no. 405.

ZELENKA, L. 1927. Geology of the area between Týn n. Vlt. and Podolsko. *Bulletin of the State Geological Institute* **7**, 479–506.

ZULAUF, G. 1994. Ductile normal faulting along the West Bohemian Shear Zone (Moldanubian/Teplá–Barrandian boundary): evidence for late Variscan extensional collapse in the Variscan Internides. *Geologische Rundschau* **83**, 276–92.

ZULAUF, G., BUES, C., DÖRR, W. & VEJNAR, Z. 2002. 10 km minimum throw along the West Bohemian shear zone: evidence for dramatic crustal thickening and high topography in the Bohemian Massif (European Variscides). *International Journal of Earth Sciences* **91**, 850–64.

ZULAUF, G., DÖRR, W., FISHER-SPURLOCK, S. C., GERDES, A., CHATZARAS, V. & XYPOLIAS, P. 2015. Closure of the Paleotethys in the External Hellenides: constraints from U–Pb ages of magmatic and detrital zircons (Crete). *Gondwana Research* **28**, 642–67.

ZWART, H. J. 1967. The duality of orogenic belts. *Geologie en Mijnbouw* **46**, 283–309.

https://doi.org/10.1017/S0016756816000030 Published online by Cambridge University Press